



# An improved model of shade-affected stream temperature in Soil & Water Assessment Tool

Efrain Noa-Yarasca<sup>1</sup>, Meghna Babbar-Sebens<sup>1</sup>, and Chris Jordan<sup>2</sup>

<sup>1</sup>School of Civil and Construction Engineering, Oregon State University, Corvallis, OR 97331, USA

<sup>2</sup>Conservation Biology Division, Northwest Fisheries Science Center (NWFSC), National Marine Fisheries Service, National Oceanic and Atmospheric Administration, 2032 SE OSU Dr., Newport, OR 97365, USA

**Correspondence:** Efrain Noa-Yarasca (enoay7@yahoo.com)

Received: 27 March 2022 – Discussion started: 23 August 2022

Revised: 4 January 2023 – Accepted: 13 January 2023 – Published: 10 February 2023

**Abstract.** Stream temperatures have been increasing worldwide, in some cases reaching unsustainable levels for aquatic life. Riparian revegetation has been identified as a strategy for managing stream temperatures by blocking direct solar radiation. In this study, the effects of riparian vegetation on stream temperatures were included within the Soil & Water Assessment Tool (SWAT) model through a shade factor parameter. An equilibrium temperature approach was used to integrate the shade factor in an energy balance context. The stream temperature sub-model was improved using the new energy balance equation and integrated into SWAT. Unlike existing models, the modified SWAT model enables improved representation of two processes – mass and heat transfer – that influence stream temperature change and enables simulation of shading and its effects on stream temperatures at sub-basin scales. The updated SWAT model was tested in Dairy McKay Watershed, OR, USA, for four scenarios: current conditions of riparian vegetation, full restoration, efficient restoration, and no vegetation. The model calibration under current riparian vegetation showed good performance (Nash–Sutcliffe efficiency  $NSE > 0.74$ ). Stream temperature reduction and number of days with stream temperatures above survival limits (NDSTASL) for aquatic species were also evaluated as measures of riparian shade performance. Findings showed average temperature reductions of  $0.91\text{ }^{\circ}\text{C}$  ( $SD = 0.69\text{ }^{\circ}\text{C}$ ) and reductions in NDSTASL of 17.1 d over a year for full riparian restoration and average reductions of  $0.86\text{ }^{\circ}\text{C}$  ( $SD = 0.67\text{ }^{\circ}\text{C}$ ) and 16.2 d for efficient restoration. Notwithstanding the similar benefits, efficient restoration was 14.4 % cheaper than full riparian vegetation restoration.

## 1 Introduction

Stream temperature is an important parameter in water quality not only because it is one of the main indicators of biodiversity and sustainable aquatic ecosystems in rivers but also because it is directly linked to other water quality parameters such as dissolved oxygen, salinity, and pH (Winfree et al., 2018; Risley et al., 2003; Brown, 1972; Poole and Berman, 2001). Ranges in stream temperature determine the habitat suitability for aquatic species. Significant changes outside the natural ranges in stream temperature can cause the death or migration of endemic species and the potential entry of non-native species, leading to an ecological imbalance (Nelitz et al., 2007; Isaak et al., 2012; Albertson et al., 2018). For example, elevated stream temperatures can increase the solubility of certain heavy metals such as cadmium, zinc, and ammonia which are toxic for aquatic life (White et al., 2017). High stream temperatures are also linked to low levels of dissolved oxygen, increases in conductivity, low levels of oxidation–reduction potential, and decreases in pH, all of which can alter aquatic life and its viability (FONDRIEST, 2014). Changes in water temperature also influence hydrological parameters such as evaporation through altering the heat flux at the air–water interface, as well as other parameters indirectly, because all processes in the water cycle are linked (Edinger et al., 1974). Historical records from the past 30 to 100 years show that stream temperatures throughout the United States have significantly increased at rates of  $0.009$  to  $0.077\text{ }^{\circ}\text{C yr}^{-1}$  (Kaushal et al., 2010). Unusual increases in water temperatures observed in the western US have exceeded limits for survival of certain aquatic species (Sherwood, 2015). For example, in the summer of 2015, the Ore-

gon Department of Fish and Wildlife estimated an approximately 55 % reduction in the sockeye salmon population along the lower Columbia River stretch due to stream temperature rising to 24.5 °C (Nguyen, 2021; Sherwood, 2015). Over the past 70 years, the abundance of species such as coho salmon has shown a drastic decline in California, with similar but less drastic trends in Oregon, due to various factors including elevated stream temperatures (NMFS, 2012, 2014). In the local area, winter steelhead, coho salmon, and resident cutthroat trout are among the primary inhabitants of the Dairy McKay watershed streams, whose population is declining due to a variety of water quality factors, including water temperature (ODA, 2018; Hennings, 2014; CWL, 2019). In this regard, the “Oregon Plan” identified salmon health as a crucial indicator of the ecosystem (ODEQ, 2001, 2008; Hawksworth, 1999; ODEQ, 2010). Additionally, in this area, declines in ecosystem structure and function have also been linked to declines in salmon numbers (ODA, 2018; Hennings, 2014).

Changes in stream temperature are driven (i) by heat transfer processes that involve the gain/loss of heat in the water body by several thermodynamic pathways and (ii) by mass transfer processes that involve the gain/loss of heat from hydrologic flows that interact and mix with the target stream (Boyd and Kasper, 2003; Chen et al., 1998a, b). Within these two types of processes, many factors corresponding to the channel morphology, hydrology, and vegetation surrounding the river affect the surface water temperature (Boyd, 1996; Winfree et al., 2018; Riskey et al., 2003). These processes can also be influenced by human activities such as the discharge of industrial effluents with high temperatures, riverbed modifications, and alteration of the riverside vegetation favoring a greater solar exposure of the water body (Hester and Doyle, 2011; Poole and Berman, 2001). While warm flow discharges from industrial effluents are the main point source of heat, shortwave radiation is the main diffuse source of heat that alters stream temperatures (Poole and Berman, 2001; Boyd and Kasper, 2003). A reduction of riparian vegetation cover can increase loading of direct solar radiation on the body of water. On the other hand, reforestation of riparian vegetation can block much of this energy before reaching the surface of the stream, thereby helping to maintain a relatively cool stream temperature (LeBlanc and Brown, 2000; Abbott, 2002; Fuller et al., 2022). To illustrate, studies conducted on the Salmon River in northern California by Bond et al. showed that simulations of partial riparian reforestation would reduce stream temperatures by 0.11 to 0.12 °C km<sup>-1</sup> and full reforestation by 0.26 to 0.27 °C km<sup>-1</sup> (Bond et al., 2015).

The increase in the temperature of streams in recent decades has stimulated the interest of researchers to study and establish predictive models. These models, mainly classified as mechanistic or statistical, vary from simple to complex, involving few to numerous parameters, with timescales ranging from minutes to months and spatial scales ranging

from local to global. Mechanistic models are physics-based numerical models involving concepts of hydrological and energy balance processes in their equations, while statistical models are models that employ data-driven techniques to establish functional relationships between stream temperature and meteorological or physical parameters of the basin (Stefan and Preud'homme, 1993; Sohrabi et al., 2017). Although statistical models may yield reliable outcomes with few parameters and simple equations (Mohseni and Stefan, 1999; Benyahya et al., 2007), they often do not consider the right physical structures that characterize the hydrological process and do not take into account the proper interaction of the hydrological process variables (Kim and Chapra, 1997; Boyd and Kasper, 2003).

Mechanistic models involve heat and mass transfer processes in their structure. Full heat transfer processes involve fluxes through the air–water interface, the water–sediment interface along the riverbed, and chemical reactions in the aquatic environment (Boyd and Kasper, 2003). However, few models have the capability to include a complete balance of heat input and output in the stream temperature simulation. Rates of gain/loss of heat from aquatic chemical reactions and through the water–sediment interface are often very small compared to heat fluxes through the air–water interface (Hebert et al., 2011). The mass transfer process requires establishing the inlet and outlet discharge flows through the water body boundaries and their corresponding temperatures. This involves knowing components from a hydrological model such as the stream tributary flows, the lateral flow, the outgoing or incoming flow rate of the groundwater, the precipitation that falls directly on the stream, and the hyporheic exchange flow (Rothwell, 2005; Ficklin et al., 2012). For example, the *Heat Source* model integrates these heat and mass transfer processes into a river-scale analytical model (Boyd, 1996; Boyd and Kasper, 2003). The *i-Tree Cool River* model is a 1D model that simulates the stream temperature including the advection, dispersion, energy flux, and mixing processes on a river scale (Abdi et al., 2020; Abdi and Endreny, 2019). Previous studies to integrate the heat transfer process into sub-basin-scale hydrologic models have resulted in models limited to certain regions and parameters, such as the Hydrologic Simulation Program–FORTRAN (Chen et al., 1998a), the Stream Network Temperature (SNTEMP) energy-balance-based model (Krause et al., 2005), the Distributed Hydrology Soil Vegetation Model (DHSVM) (Battin et al., 2007; Wigmosta et al., 1994; Yearsley, 2009), and the Hydrodynamic and Water Quality model (CE-QUAL-W2) (Zhu et al., 2019).

In the same vein, Ficklin et al. (2012) developed a hydroclimatological stream temperature model (called “Ficklin model” hereafter), within the integrated watershed model, Soil & Water Assessment Tool (SWAT; Arnold et al., 1998; Neitsch et al., 2009), which involves simplified terms representing the mass transfer process and a surrogate term representing the heat transfer process. In the mass transfer process,

the model follows a mixing approach of inflows and outflows into and out of rivers (snowmelt flow, surface runoff, lateral flow, groundwater flow – these are all SWAT model outcomes) associated with their corresponding temperatures, while in the heat transfer process it is represented by the difference between the air and water temperatures at the air–water interface multiplied by a calibrated coefficient.

Stream temperature simulations, conducted using the Ficklin et al. (2014) model in several watersheds in the Columbia River basin in northwest US (Ficklin et al., 2014); the Sierra Nevada, California (Ficklin et al., 2012); Marys River, Oregon (Mustafa et al., 2018); and Athabasca River basin in Alberta, Canada (Du et al., 2018), showed to be more accurate compared to the statistical model results proposed by Stefan and Preud'homme (1993). Although the model presents an explicit approach to the mass transfer process, including the main components of the mass balance of the river, the heat transfer process is simplified by the difference in temperature at the air–water interface multiplied by the flow travel time and the calibrated coefficient. Attempts to incorporate an explicit component of the energy balance into the Ficklin et al. model have included the use of an equilibrium temperature approach (Du et al., 2018) and the use of thermal radiation components (Mustafa et al., 2018) that are widely employed in the Heat Source model (Boyd and Kasper, 2003). These additions include a detailed representation of the heat loss/gain components through the air–water interface such as solar radiation, atmospheric longwave radiation, back radiation, convection, and evaporation. Despite efforts to include explicit energy balance in the Ficklin et al. model, they did not consider riparian vegetation in the balance equation, which is an important factor in determining stream temperature, because it blocks solar radiation from reaching the water surface features (Garner et al., 2017; Roth et al., 2010; Fuller et al., 2022). Therefore, in this work we fill that gap by incorporating riparian vegetation into the energy balance equation through the equilibrium temperature approach that characterizes the heat balance at the air–water interface (Edinger et al., 1974), and we integrated it into the Ficklin et al. stream temperature model (2012) and then incorporated it into the SWAT hydroclimatological model to improve stream temperature modeling at the sub-basin level.

Riparian vegetation has been identified as an efficient strategy to control stream temperatures by blocking solar radiation from reaching streams (Chen et al., 1998a; Roth et al., 2010; Rutherford et al., 1997). Previous studies in, for example, the USA (Abbott, 2002; Abdi et al., 2020; Chen et al., 1998b), Brazil (Ishikawa et al., 2021), Europe (Johnson and Wilby, 2015; Kalny et al., 2017; Kałuza et al., 2020), Asia (Liao et al., 2014; Liu et al., 2019), and New Zealand (Rutherford et al., 1997), among other places, have demonstrated the efficacy of riparian vegetation restoration in lowering stream temperatures. Riparian vegetation has also been shown to be effective in lowering silt and nutrients and boosting biodiversity (Malkinson and Wittenberg, 2007; Poole

and Berman, 2001). Furthermore, riparian vegetation also impacts hydrological and meteorological parameters. Prior research, for example, found that riparian plants helped to reduce wind speed and evapotranspiration in crop fields in Korean locations (Koh et al., 2010). Guenther et al. (2012) reported effects of logging on vapor pressure, wind speed, and evaporation. Rodrigues et al. (2021) also provided facts about the impact of riparian vegetation on the evaporation of reservoirs. Dugdale et al. (2018) linked riparian vegetation to changes in the flow of energy across the air–water interface and then to evaporation.

In stream temperature modeling, riparian vegetation has been represented by the shaded area over the stream generated by the canopy, in quantity, percentage of shaded area (Li et al., 2012), or shade factor (LeBlanc and Brown, 2000; DeWalle, 2010; Fuller et al., 2022). Models for determining shading or shade factor often included hydraulic and morphological properties of the river, plant characteristics in the buffer zone, and meteorological data such as solar radiation. Complex models conducted at the local scale (at specific sections of a river or short stretches of a river) even incorporated variables such as canopy shape, canopy overhang, stream bank height, canopy transmittivity, and others. Thus, these complex models also required detailed information at field level on river morphology, detailed canopy features, and in situ meteorological measurements (Davies-Colley and Rutherford, 2005; Davies-Colley et al., 2009; Li et al., 2012). However, in large stretches of rivers where information at the field level is not feasible due to limited resources, simplified models have been employed to determine the shade factor with good enough results (Fuller et al., 2022; Marteau et al., 2022; Seyedhashemi et al., 2022; Spanjer et al., 2022). In this aspect, this study takes a simplified methodology to determine the shade factor while maintaining the more representative stream and canopy features.

The main objective of this work is to add an explicit energy balance model that includes the shade factor of riparian vegetation into Ficklin's stream temperature model (Ficklin et al., 2012) and then integrate the improved approach into the SWAT hydrological model (Neitsch et al., 2009). After evaluating the improved stream temperature model in SWAT for Dairy McKay watershed (DMW) in Oregon, USA, this work also addressed the following related objectives. (1) We evaluate the effects of riparian vegetation on the shade factor and reductions in stream temperature for four scenarios: full restoration along both banks of the stream network, efficient restoration of riparian vegetation, current riparian conditions, and no vegetation. (2) We evaluate the reduction in the number of days above survival limits for aquatic species such as salmon for the two scenarios of full restoration and efficient restoration of riparian vegetation in DMW.

## 2 Materials and methods

### 2.1 Dairy McKay watershed case study

The Dairy McKay watershed (DMW) (Hydrologic Unit Code (HUC)-10: 1709001003), located in northwestern Oregon, is part of the Tualatin sub-basin (HUC-8: 17090010).

It encompasses an area of 598.3 km<sup>2</sup>, draining into the Tualatin River (Fig. 1). The DMW is characterized by higher elevations and varied topography of the Oregon Coast Range in the northern part and flat topography in the southern part. The highest elevation corresponds to 690 m a.s.l., while the lowest one corresponds to 35 m a.s.l. at the confluence with the Tualatin River. Characterized by having perennial flow, the DMW is considered one of the main tributaries of the Tualatin River, which is the prominent channel within the watershed. The major area of DMW is located across Washington County (97.4 %), with 1.3 % across Multnomah County and the last 1.3 % across Columbia County.

The DMW climate corresponds to a Mediterranean climate with a lack of rains in summer (51 mm) and mild intensity, long-duration rains in winter (719 mm). DMW soils are mainly composed of fine soils such as silt and clay with abundant natural phosphate. Despite improvements in dissolved oxygen (DO) levels in certain streams, temperatures in a significant number of streams remain above natural values (ODA, 2018; CWL, 2019). Regarding land use, there are three main areas: the northern half area is dominated by forestry, involving around 55 % of the DMW; the middle part is dominated by agriculture that encompasses around 40 %; and the southern part is dominated by a growing urban area by around 5 %. The upstream part of the DMW is dominated by long-lived trees species such as evergreen forest and shrubland, while the downstream part is dominated by seasonal crops such as Slender Wheatgrass, and at the most downstream extent it is dominated by urban areas. Due to the predominance of fine soils, upstream areas are vulnerable to erosion and landslide phenomena (Hawksworth, 1999). In agricultural areas, water quality has been found to degrade rapidly, with higher water temperature and higher phosphorus concentrations (Hawksworth, 1999; ODEQ, 2001; CWL, 2019). Some streams such as the West Fork Dairy Creek show lower DO levels than natural conditions, limiting aquatic life (ODA, 2018; Hennings, 2014).

### 2.2 Hydrologic model

Hydrological processes for DMW were simulated by using the Soil and Water Assessment Tool 2012 (Neitsch et al., 2009), developed by the United States Department of Agriculture (USDA, 2019) Agricultural Research Service (ARS). The SWAT has been utilized in watershed modeling at the sub-basin level in many places across the world with outstanding results in terms of controlling flow, erosion, nitrate, and other nutrients (Abbaspour et al., 2015; Moriasi

et al., 2007). The physics-based SWAT model is widely used to assess the impact of non-point sources, strategic conservation practices, conditions of soil management practices, and changes in land use in large and complex watersheds as well as predict their effects on flow, production of sediments and chemicals, and instream temperature (Neitsch et al., 2009). The model can simulate these hydrological processes for long periods and at daily, monthly, or annual time steps. The study area was divided into 60 sub-basins, with areas ranging from approximately 0.41 to 19.4 km<sup>2</sup> (average 9.97 km<sup>2</sup>), overlaying, as far as possible, the 12-digit HUC (Hydrologic Unit Code) boundaries from DMW, which is the US hierarchical watershed classification system. For modeling purposes, each sub-basin was divided into small areas called “Hydrologic Response Units” (HRUs), which are portions of areas that have unique combinations of slope topography, land use, and soil-type features. Slope topography was calculated from DEM (cell size 10 × 10 m) and classified into three ranges: 0 %–5 %, 5 %–20 %, and greater than 20 %. The land use and soil data were retrieved from the National Land Cover Database (NLCD) and Soil Survey Geographic Database (SSURGO) in raster format with 10 × 10 m cell size (USDA, 2019). To eliminate small coverage areas of these features into each HRU, a threshold of 10 % was considered. Hence, features with less than 10 % of its HRU area were not considered part of the combination. As a result, the SWAT model divided the DMW into 991 HRUs.

Tile drainage was considered only for agricultural areas and controlled by three parameters – depth (DDRAIN), time to drain soil to field capacity (TDRAIN), and drain tile lag time (GDRAIN), which were calibrated during flow calibration. Crop operations based on the Heat Units to maturity from the main crops (slender wheatgrass, red clover, winter wheat, sweet corn, and corn) were also considered in the watershed modeling. Stakeholders’ water rights for irrigation purposes and instream water rights were also included in the watershed modeling (OWRD, 2021). From water rights belonging to stakeholders, the allowed period to take water, the maximum volume of water allowed to take from the source, the maximum rate of water allowed to take from the source, the points of diversion (POD), and the places of use (POU) were considered in the model. From instream water rights, the minimum instream flow for irrigation diversion was considered in the model. The detailed process for including water rights in the SWAT model is available in Sect. S1 in the Supplement accompanying the article.

Precipitation and air temperature data were obtained from the PRISM Climate Group database (PRISM Climate Group, 2014). The dataset is available at a daily timescale and 4 km spatial scale. After overlaying these data, 38 data sites were found to cover the DMW area. However, points adjacent to the basin have also been considered for modeling. Thus, 58 points were considered in the SWAT model. Data on solar radiation, relative humidity, and wind speed were taken from the Forest Grove weather station

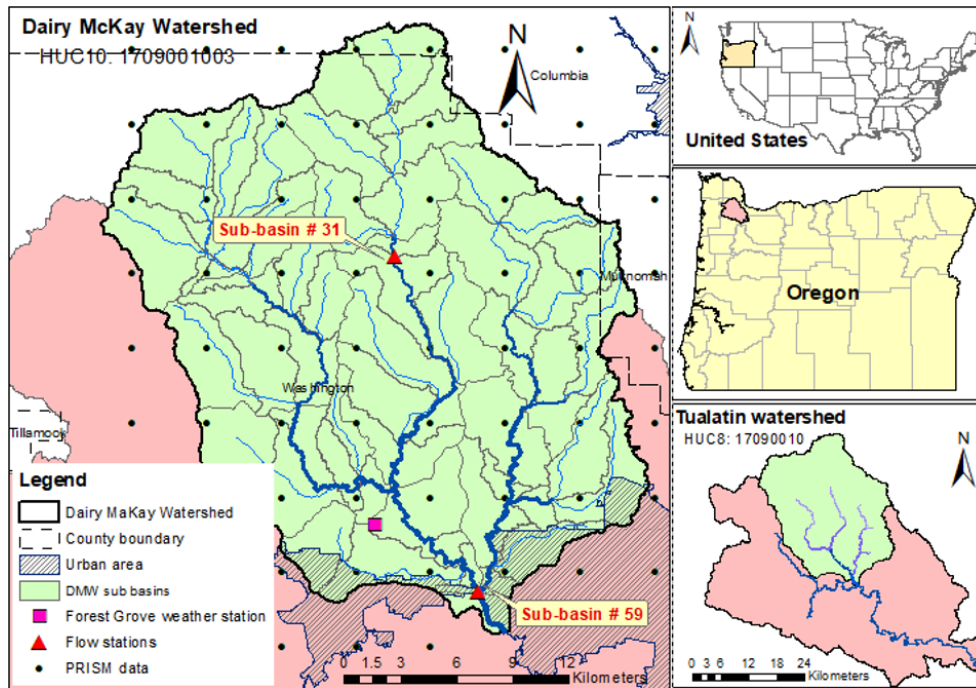


**Figure 1.** Left: streams, sub-watersheds, and political boundaries of the Dairy McKay Watershed (DMW) (HUC10-1709001003). Top right: location of DMW in the Tualatin River basin; bottom right: location of the Tualatin River basin in northwestern Oregon, USA.

(lat. 45.55305, long.  $-123.08361$ ; elevation: 54.9 m a.s.l.) from the Columbia-Pacific Northwest Region – US Bureau Reclamation dataset (USBR, 2020) on a daily timescale. Flow discharges and water temperature for calibration were obtained from two stations: the East Fork Dairy Creek near Meacham Corner (USGS 14205400) and the Dairy Creek at Route 8 near Hillsboro (station ID-14206200) (USGS). The first station lying at the sub-basin #31 outlet (see Fig. 1) was employed to calibrate the upstream DMW, while the second station lying at the sub-basin #59 outlet was employed to calibrate the downstream DMW.

### 2.3 Stream temperature model

Stream temperatures for DMW were simulated for four riparian vegetation scenarios. Scenario 1: simulation under current conditions of riparian vegetation. Scenario 2: simulation considering a full riparian restoration on both stream banks. The full riparian restoration contemplates the height of the trees equal to 45 m, which is the average height in the maturity stage (over 60 years) of the most common species in Oregon (Curtis et al., 1974). Scenario 3: simulation considering an efficient restoration of riparian vegetation. Here, in E–W- and W–E-oriented streams, the southern bank was fully restored, and the northern bank was left in its present condition. The N–S- and S–N-oriented streams were fully restored on both banks. Scenario 4: simulation under conditions of no riparian vegetation in which both banks were parameterized in the SWAT model to have zero contribution to shade factor

(SF) from vegetation. In DMW, 19 streams were classified as oriented E–W and W–E with azimuths in the range of 45 to 135° and 225 to 315°, and 41 streams were classified as N–S oriented with azimuths ranging from 135 to 225°.

#### 2.3.1 Stream temperature approach

The SWAT model by default employs a linear relationship between air temperature and stream temperature (Stefan and Preud'homme, 1993). Subsequently, Ficklin et al. (2012) proposed an improved stream temperature model via three main components that represent the mass and energy transfer processes. The first component (Eq. 1) of the Ficklin et al. model computes the local stream temperature by mixing the snowmelt flow, groundwater, surface runoff, and lateral flow and multiplying by their corresponding temperatures.

$$T_{w,local} = \frac{T_{snow}(sub\_snow) + T_{gw}(sub\_gw) + \lambda T_{air,lag}(sub\_surq + sub\_latq)}{sub\_wyld}, \quad (1)$$

where  $T_{w,local}$  is the local temperature;  $T_{snow}$  is the snowmelt temperature;  $T_{gw}$  is the groundwater temperature;  $T_{air,lag}$  is the average daily air temperature with a lag (°C);  $sub\_snow$  is the snowmelt contribution to streamflow within the sub-basin;  $sub\_gw$  is the groundwater contribution to streamflow within the sub-basin;  $sub\_surq$  is the surface runoff contribution to streamflow within the sub-basin;  $sub\_latq$  is the soil water lateral contribution to streamflow within the sub-basin;  $sub\_wyld$  is the total water yield contribution to streamflow

within the sub-basin; and  $\lambda$  is a calibration coefficient linking  $T_{\text{air,lag}}$  with  $\text{sub\_surq}$  and  $\text{sub\_latq}$ .

The second component (Eq. 2) of the Ficklin et al. model computes the temperature contribution of upstream sub-basin flow (tributary flows) to the streamflow within the targeted sub-basin.

$$T_{\text{w,initial}} = \frac{T_{\text{w,upstream}} (Q_{\text{outlet}} - \text{sub\_wyld}) + T_{\text{w,local}} (\text{sub\_wyld})}{Q_{\text{outlet}}}, \quad (2)$$

where  $T_{\text{w,initial}}$  is the stream temperature mixing the local temperature and the upstream streamflow temperature;  $T_{\text{w,upstream}}$  is the upstream stream temperature; and  $Q_{\text{outlet}}$  is the flow discharge at the outlet of the targeted sub-basin ( $\text{m}^3 \text{d}^{-1}$ ).

The third component (Eq. 3) involves terms that represent the heat transfer process and are used to adjust  $T_{\text{w,initial}}$  to obtain the final stream temperature.

$$T_{\text{w}} = T_{\text{w,initial}} + [T_{\text{air}} - T_{\text{w,initial}}] \cdot K \cdot \text{TT} \text{ if } T_{\text{air}} > 0, \\ T_{\text{w}} = T_{\text{w,initial}} + [(T_{\text{air}} + \varepsilon) - T_{\text{w,initial}}] \cdot K \cdot \text{TT} \text{ if } T_{\text{air}} < 0, \quad (3)$$

where  $T_{\text{w}}$  is the final stream temperature in the targeted sub-basin ( $^{\circ}\text{C}$ ),  $T_{\text{air}}$  is the average daily air temperature ( $^{\circ}\text{C}$ ),  $K$  is the bulk coefficient of heat transfer ranging from 0 to 1 ( $\text{h}^{-1}$ ), TT is the travel time of water through the sub-basin (h), and  $\varepsilon$  is an air temperature addition coefficient to compensate water temperatures when air temperature is negative.

### 2.3.2 Including the explicit approach of energy balance into the Ficklin et al. model

In this research, the third component of the Ficklin et al. model (Ficklin et al., 2012) was replaced by an explicit energy balance equation. Thus, the rate of heat transfer through the air–water interface of the stream is calculated as follows (Edinger et al., 1974) (Eqs. 4–5):

$$\frac{dT_{\text{w}}}{dt} = \frac{\sum H}{\rho C h}, \quad (4)$$

$$\sum H = H_{\text{s}} + H_{\text{at}} - H_{\text{b}} - H_{\text{e}} - H_{\text{c}}, \quad (5)$$

where  $\sum H$  is the sum of heat components transferred to or released by the river (net heat flux),  $\rho$  is the water density ( $\text{kg m}^{-3}$ ),  $C$  is the specific heat capacity ( $4186 \text{ J kg}^{-1} \text{ }^{\circ}\text{C}^{-1}$ ),  $h$  is the water depth (m),  $H_{\text{s}}$  is the shortwave solar radiation,  $H_{\text{at}}$  is the longwave atmospheric radiation,  $H_{\text{b}}$  is the back radiation emitted by water to the atmosphere in longwave form,  $H_{\text{e}}$  is the heat loss from water to the atmosphere through evaporation, and  $H_{\text{c}}$  is the heat gain/loss through conduction and convection. The rate of heat transfer through the air–water interface can be also represented proportional to the difference between the stream temperature and the equi-

librium temperature (Eqs. 6–8) (Edinger et al., 1974).

$$\frac{dT_{\text{w}}}{dt} = \frac{K_{\text{e}} \cdot (T_{\text{e}} - T_{\text{s}})}{\rho C h}, \quad (6)$$

$$T_{\text{e}} = T_{\text{d}}^* + \frac{H_{\text{s}}}{K_{\text{e}}} + \frac{H_{\text{at}} - 305.5 - 4.48 T_{\text{d}}^*}{K_{\text{e}}}, \quad (7)$$

$$K_{\text{e}} = 4.48 + 0.05 T_{\text{s}} + (\beta + 0.47) \cdot f(W), \quad (8)$$

where  $T_{\text{e}}$  is the equilibrium temperature defined as the hypothetical water temperature at which the net heat flux is zero, and  $T_{\text{d}}^*$  is the modified dew-point temperature. Brady et al. (1969) have found negligible loss in accuracy when the modified dew-point temperature is assumed to be equal to the original dew-point  $T_{\text{d}}^* \approx T_{\text{d}}$ ; however, in this study, the second term will be represented by a constant value (Eq. 9) that will be calibrated.

$$T_{\text{d}}^* \approx T_{\text{d}} + c_0 \quad (9)$$

For air temperatures ranging from 0 to 30  $^{\circ}\text{C}$ , the relationship between the air and dew-point temperature is nearly linear. Considering that more than 97 % of the DMW air temperature over a year is within this range (0–30  $^{\circ}\text{C}$ ), we can assume a linear relationship between the air and the modified dew-point temperature (Parish and Putnam, 1977) (Eq. 10).

$$T_{\text{d}}^* \approx C_1 T_{\text{a}} + C_2, \quad (10)$$

where  $C_1$  and  $C_2$  are constants to be calibrated in the model. However, since the dew point is always lower than or equal to the air temperature, the coefficients were constrained to get  $T_{\text{d}} < T_{\text{a}}$ .

The shortwave radiation reaching the water surface is equal to the difference between the potential solar radiation and the radiation blocked by barriers such as topography and riparian vegetation. This difference can also be expressed in terms of the shadow that the barriers generate over the streams as a factor (Boyd and Kasper, 2003; Abdi et al., 2020) (Eq. 11).

$$H_{\text{s}} = 0.97 H_{\text{day}} (1 - \text{SF}), \quad (11)$$

where  $H_{\text{day}}$  is the incident total solar radiation per day ( $\text{MJ m}^{-2} \text{d}^{-1}$ ), and SF is the shade factor.

The longwave radiation ( $H_{\text{at}}$ ) emitted by the atmosphere is computed by the Stefan–Boltzmann law (Hebert et al., 2011; Morin and Couillard, 1990; Kim and Chapra, 1997).

### 2.4 Shade factor approach

The shade factor was calculated as the portion of solar radiation blocked by the topography and riparian vegetation divided by the potential solar radiation that would reach the stream surface (Boyd and Kasper, 2003). Thus, the shade factor varied from 0 (when no solar radiation is blocked) to 1 (when all the potential solar radiation heading toward

the stream is blocked). The amount of radiation blocked by the barriers depended on the size and proximity of trees, topographic angle, solar azimuth, solar angle, stream width, stream azimuth, stream coordinates, the percentage of solar radiation that penetrates the canopy, and date/time. Thus, the shade factor was different for each stream, each day within the year, and each instant within the day. This calculation process was performed in the Python environment (available at [https://github.com/noayarae/SF\\_model.git](https://github.com/noayarae/SF_model.git), Noa-Yarasca, 2021), and then the results were input into the SWAT hydrological model.

The existing vegetation height (EVH) data were obtained from the Land-fire Program (LP) database (LANDFIRE, 2019) in raster format with  $10 \times 10$  m cell size. The average height in a 30 m buffer was obtained. The proximity of trees was assumed constant and equal to 5.0 m, which is approximately equal to the average crown radius of the major tree species of Oregon at maturity (Bechtold, 2003; Temesgen et al., 2007). Since forests and riparian vegetation in DMW were mostly evergreens (LANDFIRE, 2019) that keep their leaves year-round and maintain a nearly constant high average leaf area index throughout the year (Thomas and Winner, 2000; Ishikawa et al., 2021), the shade factor did not consider seasonal changes in the leaf area index of riparian vegetation. For the scenarios of full and efficient riparian restoration, we also assume that this type of vegetation will be planted. However, in rivers buffered by other types of vegetation, seasonal defoliation may be relevant to consider.

The topographic angle, measured between the middle of the stream and the highest topographic feature in a radius of 50 km, was calculated from the DEM in the GIS environment for each river and each solar azimuth. When the topographic angle was greater than the riparian vegetation angle, the blocked solar radiation was assigned to the topography.

Thus, the SF has been calculated for each day of the temperature simulation period and for each DMW stream. To simplify, assumptions about the geometry have been considered (Li et al., 2012). The SF estimate did not consider, for example, the geometry of the trees or the density of the riparian vegetation. The detailed process for calculating the shade factor is available in Sect. S2 in the Supplement.

## 2.5 Model calibration setup

Flow and stream temperature calibration processes were performed at East Fork Dairy Creek and at Dairy Creek on Route 8 station, which are outlets of the sub-basin #31 and sub-basin #59, respectively. SWAT-CUP (Soil & Water Assessment Tool – Calibration Uncertainty Program) was used to calibrate the flow by changing 17 parameters (details of the calibrated parameters are available in Sect. S3). Flow calibration was carried out in sub-basin #31 (upstream of the DMW) from 1 January 2006 to 31 December 2018 and in sub-basin #59 (downstream of the DMW) from 5 May 2011 to 31 December 2018. The calibrated parameters in sub-basin

#31 were extended to the other upstream sub-basins with similar physical characteristics to sub-basin #31, while the calibrated parameters in sub-basin #59 (downstream) were extended to downstream sub-basins. On the other hand, the proposed stream temperature model was calibrated at the outlet of sub-basin #31 from 16 February 2012 to 31 December 2008 and at the outlet of sub-basin #59 from 1 January 2006 to 5 March 2012. The calibration was accomplished by an iterative procedure that was systematized in Python code following the steps shown in Tables S4 and S5 in Sect. S6 in the Supplement. The Python code to iteratively run SWAT, the input data, required SWAT files, and the modified SWAT model (in Fortran) may be found in the Zenodo repository at <https://doi.org/10.5281/zenodo.6301709> (Noa-Yarasca, 2022). Calibration was carried out by changing four parameters ( $\lambda$ ,  $t_{air\_lag}$ , which are parameters from the pre-determinate Ficklin et al. model, and  $C_1$  and  $C_2$ , which are coefficients introduced in this study). Following the Latin hypercube sampling criterion (Iman, 2014), 2000 sample sets of the four coefficients ( $\lambda$ ,  $t_{air\_lag}$ ,  $C_1$ , and  $C_2$ ) were generated and iteratively evaluated to find the optimal values of the parameters.

## 2.6 Model calibration evaluation

The model's efficiency was assessed using the Nash–Sutcliffe efficiency (NSE) criteria, which is given by the equation below.

$$NSE = 1 - \frac{\sum_{i=1}^n (O_i - S_i)^2}{\sum_{i=1}^n (O_i - O_{avg})^2}, \quad (12)$$

where  $O_i$  is the observed value at time  $i$ ;  $S_i$  is the modeled value at time  $i$ ; and  $O_{avg}$  is the mean of observed values. NSE values range from  $-\infty$  to 1, with 1 indicating a perfect model with zero prediction error,  $NSE = 0$  indicating a model with predictive power equal to the mean of observed values, and negative values indicating a very severe model error with prediction worse than the mean of observed data. Previous research has classified models with NSE values less than 0.5 as unsatisfactory, models with values more than 0.65 as good, and models with values greater than 0.75 as very good (Moriassi et al., 2007).

In addition, the average tendency of the simulated values to be greater or lower than their observed values was measured by percent bias (PBIAS), given by

$$PBIAS = 100 \frac{\sum_{i=1}^n (O_i - S_i)}{\sum_{i=1}^n O_i}, \quad (13)$$

where  $O_i$  is the observed value at time  $i$  and  $S_i$  is the modeled value at time  $i$ . PBIAS has an optimum value of 0, with values close to zero suggesting accurate model simulation. Positive values imply overestimation bias, whereas negative values suggest underestimating bias in the model.

Moreover, model error was evaluated using the mean absolute error (MAE), given by

$$\text{MAE} = \frac{1}{n} \sum_{i=1}^n |S_i - O_i|. \quad (14)$$

This is an arithmetic average of the absolute errors between paired observed and simulated values. The MAE ranges from 0 to  $\infty$  in the same units as the target variable (temperature – °C). Given that it is a negatively oriented score, models with low MAE are preferable, with MAE = 0 being the ideal model.

### 3 Results and discussion

#### 3.1 Flow calibration

For flow, the calibrated model achieved a Nash–Sutcliffe efficiency (NSE) of 0.74 for sub-basin #31 and 0.86 for sub-basin #59. The PBIAS values obtained were 8.9 % for sub-basin #31 and 6.4 % for sub-basin #59. These efficiency values are consistent with calibrations performed for other watersheds (Moriassi et al., 2007; Arnold et al., 2012), in which the NSE for the flow calibration ranged between 0.58 and 0.98 and the PBIAS was less than 10 %. Figure 2a and b shows the performance of the calibrated model.

#### 3.2 Stream temperature calibration

##### 3.2.1 Shade factor

The shade factor in the DMW streams varied both temporally and spatially. Temporally on average, the shade factor in winter was found to be greater than in summer. Spatially, the shade factor ranged from 0.001 in streams with very little riparian vegetation to 0.91 in streams with existing vegetation with tall trees. Note that values of shade factor for each stream for the existing vegetation and other scenarios have also been graphed and are discussed in more detail in Sect. 3.3.1. In addition to existing vegetation and topography, the temporal variation of the SF was driven by variation in solar declination and solar azimuth during the year, while the spatial variation of SF was driven primarily by stream orientation. Thus, the contribution of riparian vegetation and topography in blocking the solar radiation, and therefore in the shade factor, was mainly conditioned by the stream orientation (varying spatially), solar declination, and solar azimuth (varying temporally).

Overall, the contribution of topography to the shade factor was found to be small compared to the contribution of riparian vegetation. For example, considering that the SF goes from 0 to 1, the topography contribution was found to be from 0.001 to 0.08, while the riparian contribution was found to be from 0.01 to 0.87. The contribution of topography to SF was found to be even lesser in downstream streams

than in upstream streams. For example, the average contribution of topography in the SF in upstream streams was 0.04, while in downstream streams it was 0.004. This means that the amount of solar radiation blocked by the topography was considerably less than the amount blocked by the riparian vegetation in this watershed; however, in rivers surrounded by high ridges, the topographic contribution may be more relevant.

Regarding riparian vegetation, as the DMW is located in the Northern Hemisphere, solar declination greatly favored the southern bank riparian vegetation to shade E–W- and W–E-oriented streams rather than the northern side. Therefore, the southern bank contribution to the SF was significantly greater than that of the northern bank in E–W- and W–E-oriented streams. However, in streams located in the Southern Hemisphere, this contribution would be inverse. In N–S- and S–N-oriented rivers, the contributions of riparian vegetation from the western and eastern banks to the SF were similar over the year.

##### 3.2.2 Calibration

The values of the four calibrated coefficients ( $\lambda$ ,  $t_{air\_lag}$ ,  $C_1$ , and  $C_2$ ) driving the modified stream temperature model were 0.88, 5, 0.67, and 1.16 for sub-basin #31 and 1.06, 6, 0.74, and 1.17 for sub-basin #59, respectively. The Nash–Sutcliffe efficiency (NSE) values for sub-basin #31 and #59 were 0.74 and 0.82, respectively. These two NSE values are considered good fit and very good fit (Moriassi et al., 2007), respectively, and are consistent with successful calibrations reported in other studies ranging from 0.70 to 0.89 (Ficklin et al., 2012; Mustafa et al., 2018; Du et al., 2018). Figure 3a and b shows the performance of the calibrated model. Although the calibration achieved encouraging evaluation coefficients, the gap between observed and simulated values during the winter at the upstream control point (sub-basin #31) is notable compared to other periods. In this period and zone, the stream temperature may be influenced by additional factors or variables that have not been considered in this study. These factors can be, for example, canopy density changes in winter, hyporheic flow, heat from winter precipitation, bottom friction heat in winter flows, and others. Future research is recommended to take these aspects into account.

The stream temperature calibration using the modified Ficklin et al. model highly outperformed stream temperatures computed by using Stefan's equation (linear model currently used as the default approach in SWAT). On the other hand, the accuracy of the modified model was found to be fairly similar (within  $\pm 0.05$  NSE of each other) to the original Ficklin et al. model (Table 1). Residual values of stream temperature simulated by the linear model, calibrated by the original and the modified Ficklin et al. model for sub-basin #31 and sub-basin #59 are also shown in Fig. 4a and b.



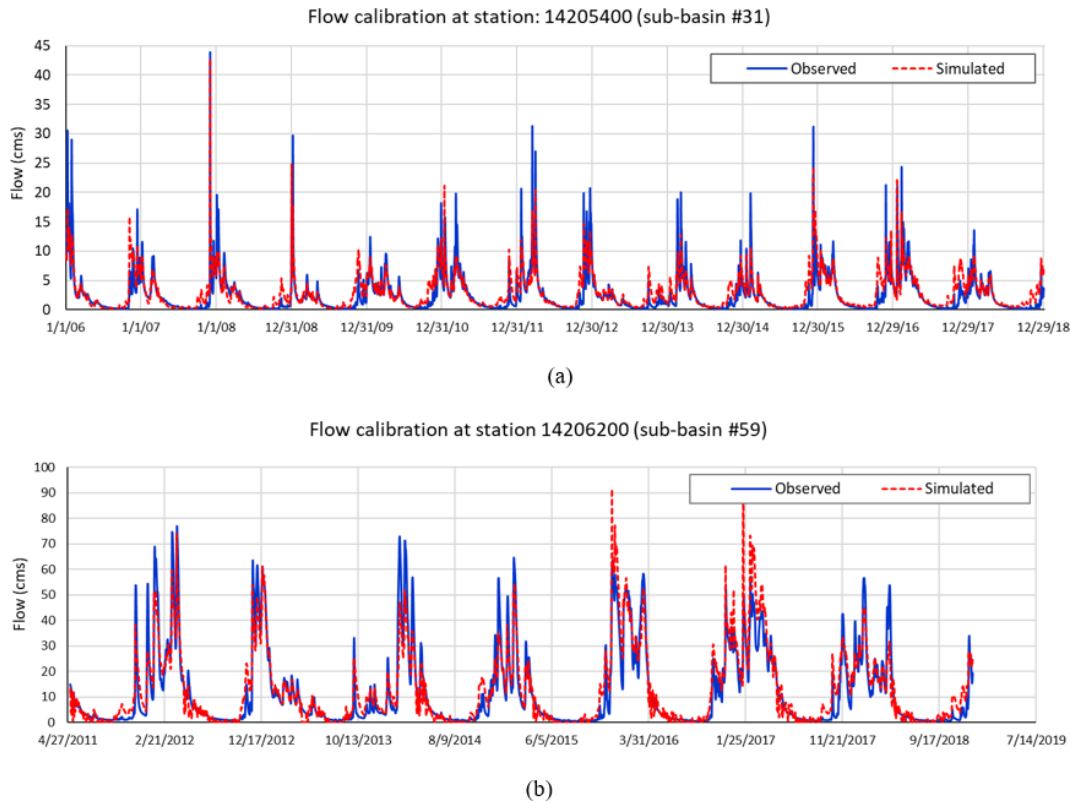


**Figure 2.** (a) Flow calibration at station USGS-14205400 (outlet of sub-basin #31) and (b) station 14206200 (outlet of sub-basin #59).

**Table 1.** Calibration coefficients for the linear, original Ficklin et al., and modified Ficklin et al. stream temperature models.

| Calibration site | Modified Ficklin et al. stream temperature model |        |          | Original Ficklin et al. stream temperature model |        |          | Linear stream temperature model |        |          |
|------------------|--|--------|----------|--|--------|----------|---------------------------------|--------|----------|
|                  | NSE  | PBIAS  | MAE (°C) | NSE  | PBIAS  | MAE (°C) | NSE                             | PBIAS  | MAE (°C) |
| Sub-basin #31    | 0.74   | -8.2 % | 1.65     | 0.77   | -3.6 % | 1.41     | 0.46                            | 22.8 % | 2.47     |
| Sub-basin #59    | 0.82   | -4.4 % | 1.40     | 0.85   | -3.1 % | 1.31     | 0.7                             | 20.4 % | 2.28     |

### 3.3 Evaluating the effects of riparian vegetation on stream temperature

Data of existing vegetation of the main DMW streams show 45.3 % of non-forested banks, 42.5 % of partially forested banks, and only 12.2 % of highly forested banks, indicating that there is still a significant area of buffer zone to reforest and an important amount of solar radiation heading to the streams to be blocked. However, the restoration of all potential vegetation can become a costly alternative as financial resources are often limited (Minnesota Board of Water and Soil Resources, 2009). Hence, the optimization of potential riparian restoration then results to be an effective option to find the most favorable riparian restoration without sacrificing the goal of stream temperature reduction.

#### 3.3.1 Effects of riparian vegetation on the shade factor

The full (scenario 2) and efficient (scenario 3) riparian restoration resulted in increases in the shade factor (SF) with respect to the existing riparian vegetation (scenario 1) in all 60 DMW streams (Fig. 5). In streams with no forested and partially forested banks, substantial SF increases were obtained. For example, the SF of stream #20 in sub-basin #20 increased from 0.002 (current SF) to an average of 0.93 under full reforestation and to 0.86 under efficient reforestation. In areas forested with relative tall trees, minor increases in SF have been obtained. For example, the SF of stream #1 increased from 0.82 (current SF) to 0.89 (in full and efficient riparian reforestation).

The contribution of riparian vegetation in the SF varied according to the stream orientation (azimuth) and the stream bank. To illustrate, in stream #20 (with azimuth 107.5° –

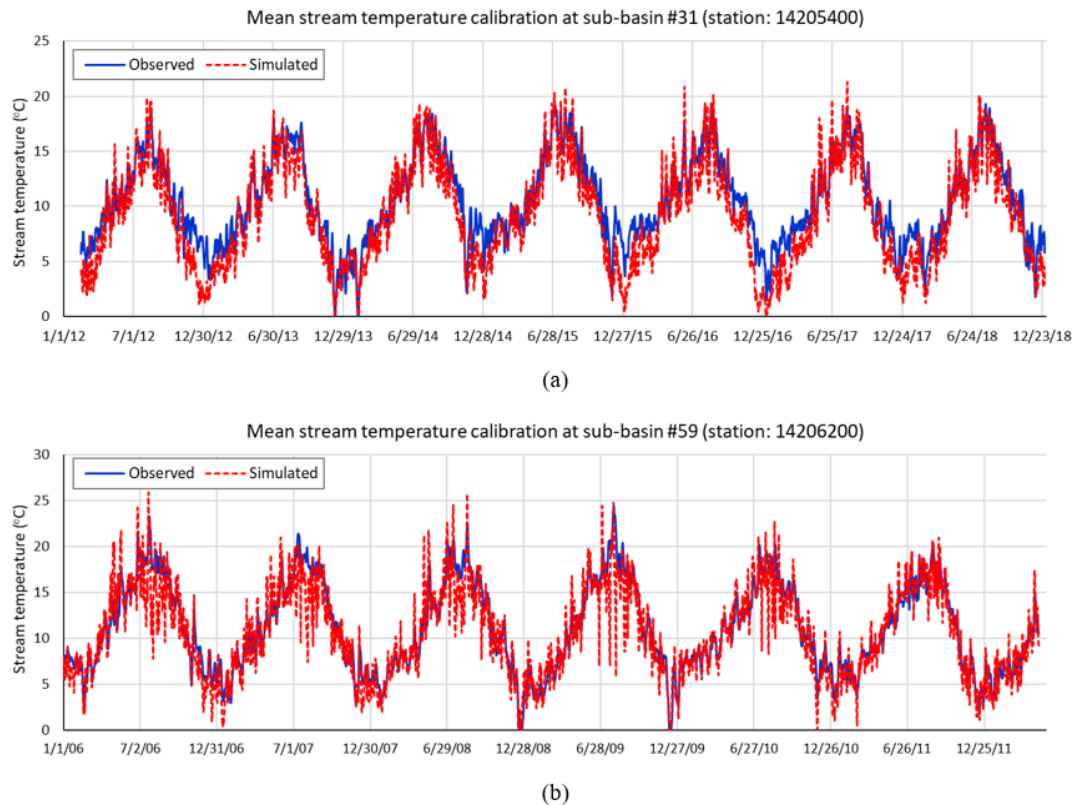


**Figure 3.** (a) Mean stream temperature calibration at USGS-14205400 station (outlet of sub-basin #31) and (b) station 14206200 (outlet of sub-basin #59).

near W–E orientation), in full riparian restoration, the southern bank contributed 92.2% in the SF increase, while the northern bank contributed in only 7.7%, and the topography contribution was 0.1%. In efficient riparian restoration (scenario 3), the northern bank was not considered reforested; therefore, the SF increase is only due to the southern bank reforestation.

Overall, due to DMW’s location in the Northern Hemisphere (Fig. 1), in streams with dominant E–W and W–E orientations, the contribution to SF from the southern-side riparian vegetation was greater than that from the northern side. In streams with dominant N–S and S–N orientations, the contributions to SF from the eastern- and western-side riparian vegetation were similar. Details showing the contribution of stream banks to the SF increase are available in Sect. S4.

### 3.3.2 Reduction of mean stream temperature

The full and efficient riparian restoration resulted in stream temperature reductions with respect to the existing riparian vegetation in all 60 DMW streams. In both riparian restoration scenarios, average annual temperature reductions in stream segments ranged from 0.02 to 3.17°C compared to current conditions (scenario 1). Despite the same ranges, the mean reduction in stream temperatures for full riparian

restoration was 0.91°C (SD = 0.69°C), while for efficient restoration it was 0.86°C (SD = 0.67°C). In the summer period, these reductions ranged between 0.03 and 5.21°C, with a mean of 1.40°C (SD = 1.17°C) for full riparian restoration and 1.31°C (SD = 1.13°C) for efficient riparian restoration (Fig. 6a and b). Reductions in stream temperature were found to be directly proportional to increases in shading factor. Thus, streams with substantial increases in SF also showed substantial reductions in stream temperatures.

As in the SF analysis, in streams with dominant E–W and W–E orientations, the contribution to stream temperature reduction of riparian vegetation on the southern side was greater than that on the northern side. In N–S- and S–N-oriented streams, both the eastern and western banks contributed to the stream temperature reduction in a similar way. Details showing the contribution of stream banks to the stream temperature reduction are available in Sect. S5. Stream temperature reductions for full and efficient riparian restoration were quite similar. This implies that a strategic allocation of riparian vegetation can achieve levels of stream temperature reduction as well as a full restoration. This finding is consistent with previous studies seeking strategic placement of riparian vegetation to achieve the greatest reduction in water temperature. DeWalle (2010), for example, discovered that during summer solstice south-bank ri-

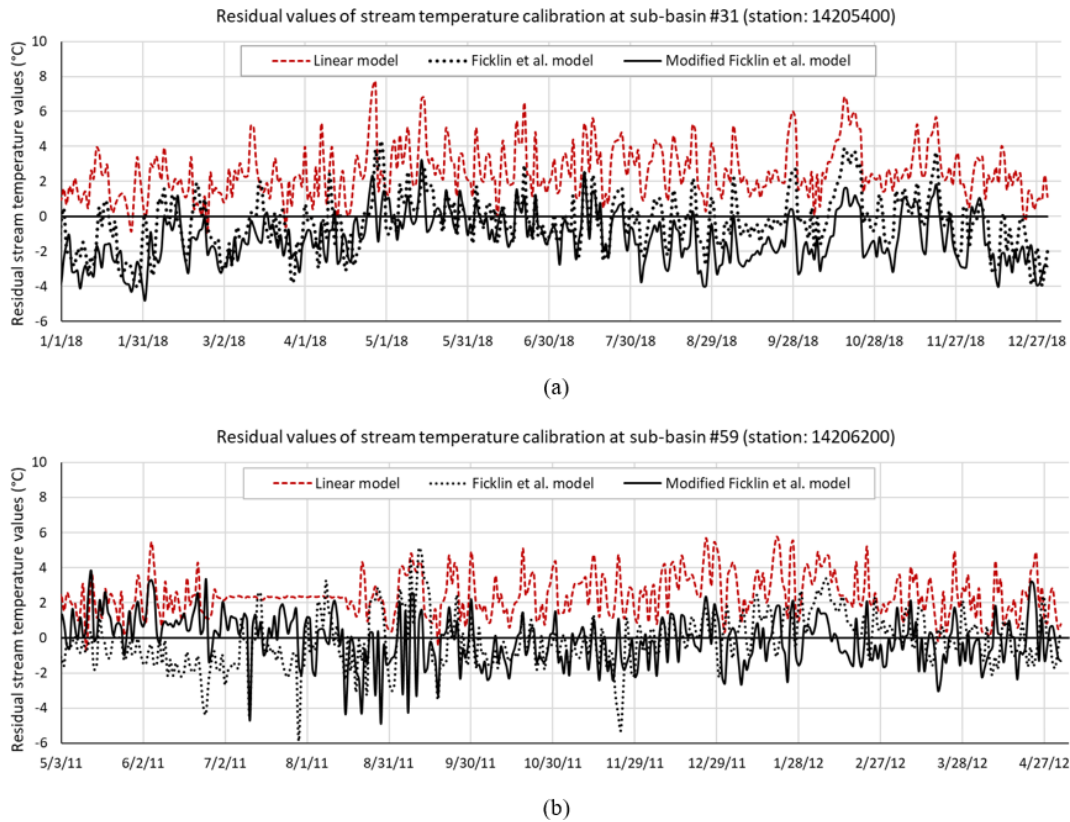


**Figure 4.** Residual values of stream temperature simulated by the linear model, calibrated by the original and the modified Ficklin et al. model for (a) sub-basin #31 and (b) sub-basin #59 for the last year of the calibrated period.

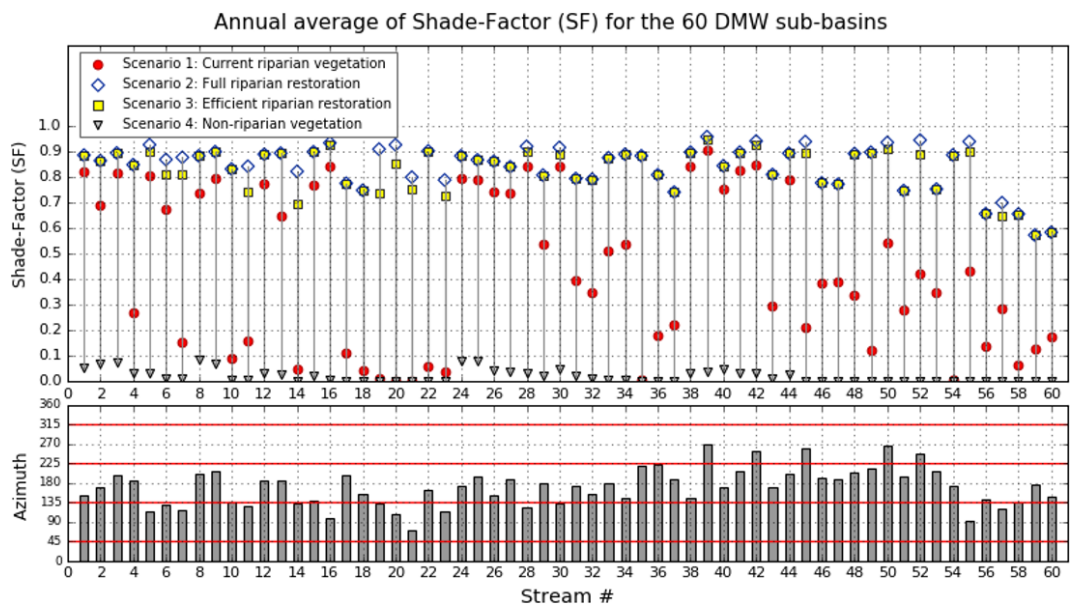


**Figure 5.** Annual average of shade factors (SFs) for the 60 DMW streams for scenarios 1, 2, 3, and 4.

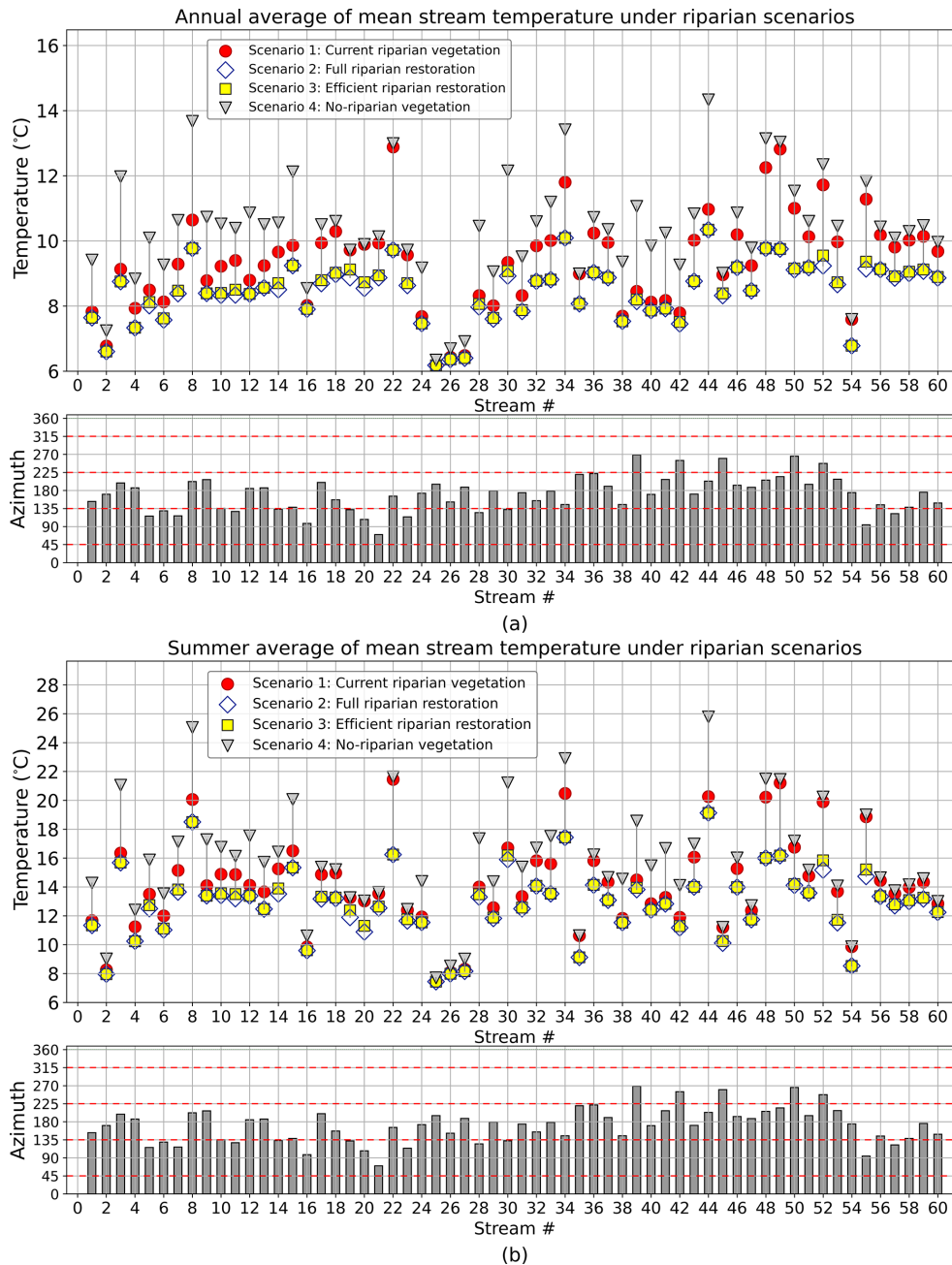


**Figure 6.** Result of mean stream temperature simulation for scenarios 1, 2, and 3. **(a)** Annual average of stream temperature. **(b)** Summer average of stream temperature.

riparian vegetation in E–W streams produced 70 % of total daily shade compared to 30 % of north-bank vegetation on a 40° N stream, while in N–S streams’ shading from both banks was equivalent. Similarly, Garner et al. (2017) reported that planting on the southernmost bank of Northern Hemisphere streams flowing E–W, NE–SW, or NW–SE (and vice versa) would result in optimal planting targeted at cooling stream water due to its greater contribution in shadowing compared to the northern bank. Likewise, Jackson et

al. (2021) found that in E–W/W–E-oriented rivers the contribution of the north-bank riparian vegetation was negligible when compared to the south bank. Thus, tree planting on the north side may be unnecessary for stream temperature control. In N–S/S–N-oriented streams, the riparian vegetation on both sides had the same shading effect on streams.

### 3.3.3 Reduction of the number of days with 7 d average maximum stream temperature greater than 18 °C

The 7 d average maximum (7dAM), calculated by averaging the daily maximum stream temperatures for 7 consecutive days, is the biologically based numeric temperature criterion to characterize the beneficial use of freshwater (ODEQ, 2008). To evaluate the model performance in relation to biological criteria, we used the numeric temperature criteria corresponding to salmon and trout rearing migration, which establish that the 7dAM values do not exceed 18 °C (ODEQ, 2008). In full riparian restoration, the reduction of the number of days exceeding 18 °C over the year on average varied from 0 to 58.5 d ( $M = 17.1$ ) (Fig. 7a) and over the summer from 0 to 33 d ( $M = 11.4$ ) (Fig. 7b). The lowest reduction was observed in stream #25, while the greatest reduction was observed in stream #49. In efficient riparian restoration, the reduction of the number of days exceeding 18 °C over the year and over the 60 DMW streams varied from 0 to 58.5 d ( $M = 16.2$ ), and over the summer it varied from 0 to 29.4 d ( $M = 10.6$  °C), on average. These reductions were consistent with the increase of the SF. In the sub-basins with higher SF increases, the reduction values of the number of days exceeding 18 °C were also found to be higher.

Previous studies have also obtained positive relationships between increased riparian vegetation and reduced stream temperature using various metrics (Wondzell et al., 2019; Parkyn, 2004; Kalny et al., 2017; Abbott, 2002; Garner et al., 2017). However, given that future climate change scenarios foresee prolonged hot days that would affect aquatic life (Brander, 2007), this work presents the reduction of days with 7dAM that exceed 18 °C, which could be a more practical value/metric for experts and non-experts. The reduction in the number of days with 7dAM indicates encouraging findings for DMW; nevertheless, it was not able to compare with earlier research, since those studies directly concentrate on temperature reduction under various conditions.

### 3.3.4 Cost of riparian restoration

Considering the vegetation density data in a 30 m buffer zone, approximately 1900.7 acres of non-forested areas and 1770.6 acres of partially forested areas could be restored in the DMW. Riparian restoration costs vary according to factors such as location and technology used. In 2010, the ODEQ estimated the average cost of restoring riparian vegetation in rural areas at USD 4695 per acre (ODEQ, 2010). Based on the cost value estimated for 2010, the full riparian restoration of DMW streams could cost USD 12.27 million, while an efficient riparian restoration could cost USD 10.51 million. Therefore, the efficient riparian restoration could be 14.4 % cheaper in cost than the full restoration, while in terms of benefits of reducing stream temperature and reducing the number of days exceeding 18 °C, efficient restoration would have achieved more or

less similar results to full restoration. Using the reduction in the number of days exceeding 18 °C as a metric for benefit of riparian restoration, the benefit–cost ratio (BCR) was determined as an indicator of investment efficiency in the 60 DMW streams (Fig. 8). The BCR values show that headwater streams obtain greater benefits from riparian vegetation restoration per investment cost than downstream streams in both full restoration (scenario 2) and efficient restoration (scenario 3) (Fig. 9a and b). The detailed process for calculating the cost of riparian restoration/reforestation is available in Sect. S7.

### 3.3.5 Evaluating additional effects of riparian vegetation for optimal restoration (future research)

In addition to the positive impacts of riparian vegetation on stream temperature reduction revealed here and earlier research (Abbott, 2002; Roth et al., 2010; Garner et al., 2017; Kalny et al., 2017; DeWalle, 2010; Sahatjian, 2013), other impacts should not be overlooked when evaluating the implementation of buffer vegetation. Riparian vegetation has also been linked to other services such as reducing nutrients in streams caused by agricultural and livestock activity (Groh et al., 2020; Lutz et al., 2020), controlling soil erosion and bank stability (Dickey et al., 2021), and controlling storm runoff by slowing down water contribution to streams, absorbing rainwater, and allowing groundwater recharge, among others (Hawes and Smith, 2005). While water temperature regulation is based on the canopy's capacity to block solar radiation, other riparian-vegetation services are linked to plant functional features such as root absorption capability, root density, and root depth. The efficient restoration of riparian vegetation reported in this work does not necessarily imply effective restoration for other purposes (nutrient reduction, flow, and erosion control), since these other services are related not only to the canopy but also to other plant functional properties (Malkinson and Wittenberg, 2007; Hawes and Smith, 2005).

A riparian buffer consisting of a mix of trees, shrubs, and grasses is much more efficient in removing a broad range of contaminants than a riparian buffer consisting primarily of trees. This is because grasses' shallow and dense roots are excellent in slowing overland flow and trapping sediments, whereas tree roots are good at absorbing nutrients from groundwater, stabilizing banks, and regulating streamflow (Hawes and Smith, 2005). Furthermore, trees provide shade to cool the water and habitat for birds and other wild critters, and falling leaves and branches provide a source of food for wildlife and aquatic animals. Thus, grasses and shrubs can provide services that forests cannot (Parkyn, 2004).

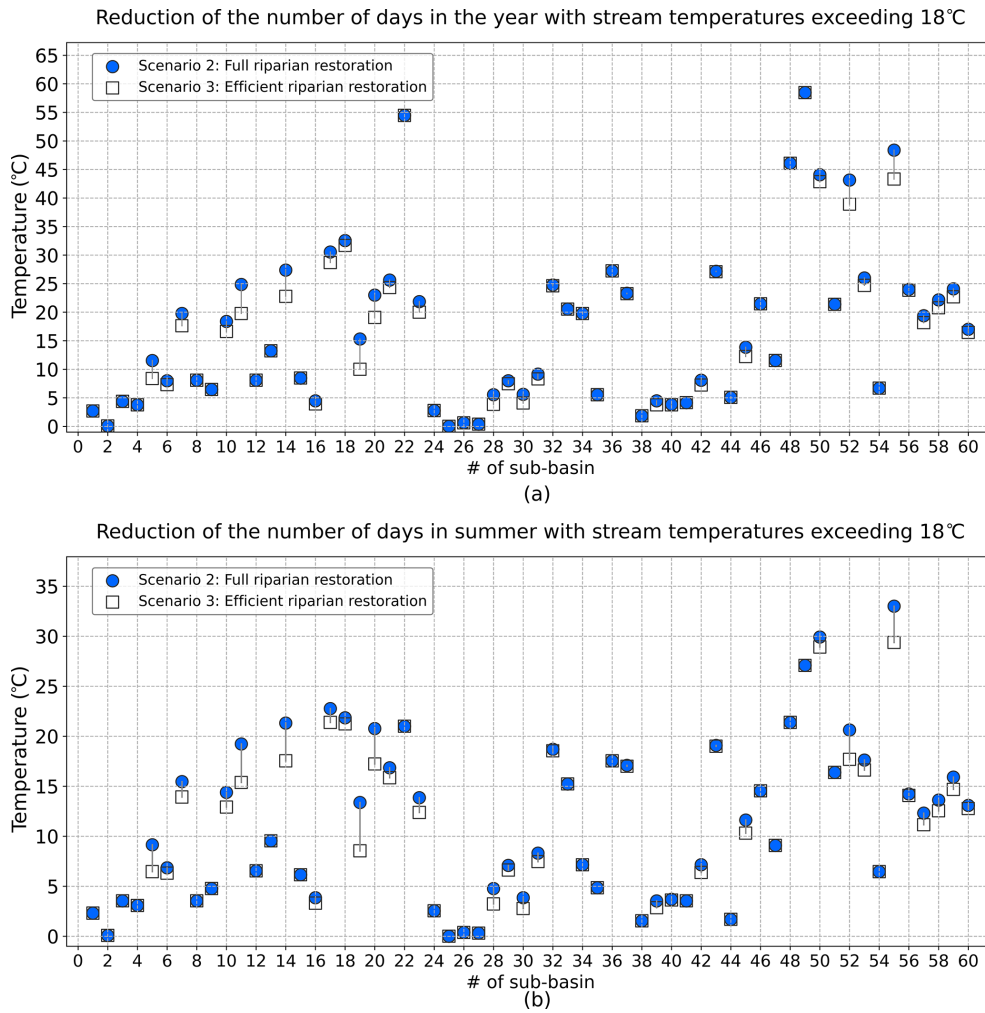


**Figure 7.** Reduction of number of days in (a) the year and in (b) summer with 7dAM stream temperatures exceeding 18°C in scenarios 2 and 3.

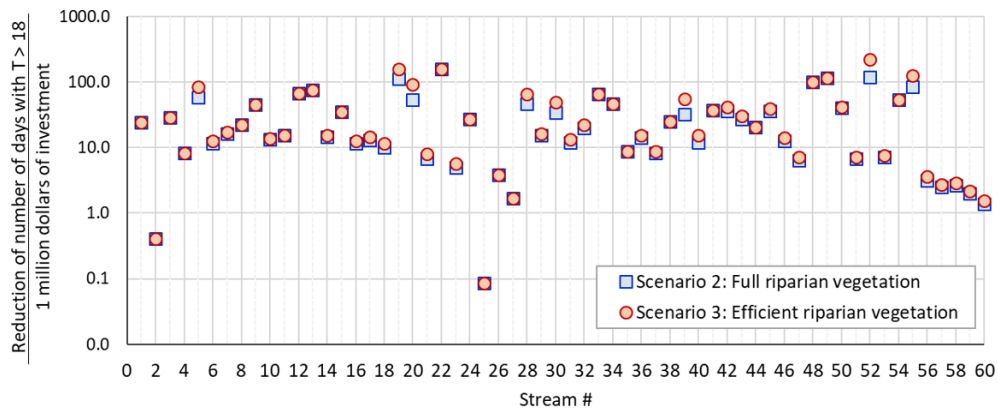


**Figure 8.** Benefit–cost ratio (reduction of the number of days that exceed 18°C per cost of the riparian restoration in millions of dollars) for the 60 DMW stream for the case of full riparian restoration (scenario 2) and efficient riparian restoration (scenario 3).

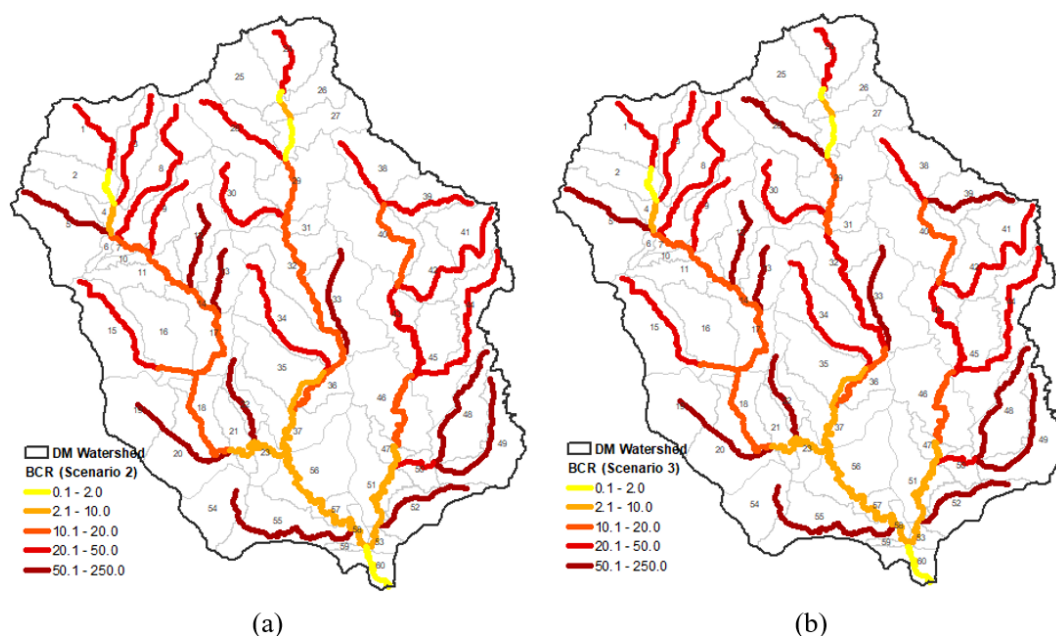


**Figure 9.** (a) Benefit–cost ratio map for full riparian restoration (scenario 2). (b) Benefit–cost ratio map for efficient riparian restoration (scenario 3). The reduction in the number of days that exceed  $18^{\circ}\text{C}$  was considered a riparian restoration benefit. The cost corresponds to the 2010 riparian restoration cost in millions of dollars.

On the other hand, fully riparian vegetation restoration may greatly increase transpiration on hot days, resulting in greater water extraction from rivers by plants, which may be temporarily detrimental to sensitive aquatic species (Hernandez-Santana et al., 2011; Garner et al., 2017). Furthermore, heavy shade could affect the population of primary food producers such as periphyton and grazing snails (which are important oxygen providers for secondary consumers), water quality regulators, homes of tiny creatures, and soil moisture reservoirs (National Park Services, 2020; Schiller et al., 2007; Hill et al., 1995).

If riparian vegetation could be planted along the entire length of the river, the main expected impact would be a reduction in nutrients, sediments, overflows, and stream temperature in various measures, as well as changes in certain sub-processes of the water cycle in the river environment such as transpiration and aquifer recharge, among others. Other expected consequences include the loss of some primary food producers, which may affect the food chain near the river. The findings of effective riparian vegetation restoration in this work are focused on a single goal: stream temperature. These results may vary in a multi-objective assessment of riparian vegetation restoration. Further work is encouraged to assess and evaluate the implementation of multi-target riparian vegetation.

### 3.3.6 Model limitations and uncertainties

Although this study achieved encouraging findings in terms of stream temperature decrease through the implementa-

tion/restoration of riparian vegetation, it should be noted that these results may vary due to the uncertainty that the proposed model entails. The stream temperature model outcomes are subject to uncertainties arising from sources, such as input data, model structure, and model parameters.

The input data included hydrometeorological observations (air temperature, wind speed, solar radiation, and humidity), surface (land cover, vegetation height), and subsurface watershed features (groundwater properties), among others, that were mainly obtained from open-source repositories on the internet. Land cover and riparian vegetation (important component in this work), for example, are derived from preprocessed satellite measurements. Despite significant improvements in remote sensing measurement techniques, errors and uncertainties remain when adapting these data to the model. For example, raster vegetation data with a cell size of  $10 \times 10\text{ m}$  weights land cover features that are not necessarily uniform within the cell area. Furthermore, remote sensing reads the vegetation at different time intervals and interpolates/extrapolates or weights it for the entire year or certain seasons of the year; yet, the vegetation is dynamic at all times. In reference to solar radiation, for example, given the limited number of measurement locations, the Forest Grove station's records for solar radiation were extended over the whole DMW. Despite the short range of latitudes and longitudes, which could assume uniform solar radiation in the DMW, variables like cloud cover would make this variable changeable in space. Furthermore, to calculate the daily shade factor by integrating instantaneous shade factors

(0.01 h), the available daily solar radiation was downscaled using models available in the literature, which also carried uncertainty.

The temperature model also included several parameters, coefficients, and constants where, despite our meticulous and judicious selection and assumption of these parameters, the certainty of many of them could not be verified directly but had to be assumed based on the similarity of our case of study with the cases for which they were obtained. This inevitably generated another source of uncertainty in the proposed model. Among these parameters are, for example, the coefficients of the various thermal sources in Edinger's (1974) equilibrium temperature equation and the coefficients of the Ficklin equation, which, while some of them were calibrated, could not be homogeneous throughout the DMW. In terms of parameter calibration, this was performed during the relatively short time of data available for flow and stream temperature; however, a calibration over a longer period might modify the calibrated parameter values and hence the model outcomes.

With respect to structure uncertainty, the equilibrium temperature model assumes simplifications to facilitate calculation and overcome some limited resources. Among these is the linearization of the quartic energy balance equation, which in its original form is challenging to manipulate and incorporate into the hydrological model. Furthermore, based on Brady et al. (1969) and Lawrence's (Lawrence, 2005) proposal, the relationship between air and dew-point temperature reduces to a linear equation, indicating that errors with this assumption may be ignored.

Finally, as with any modeling process, this work attempted to gather and preprocess high-quality input data, assumed parameters using physical criteria, and simplified certain equations to facilitate stream temperature modeling and integrate it into the hydrological model, but these efforts inevitably introduced uncertainties. Findings of this study are limited to the ranges used here, as well as the DMW characteristics. Future research should continue exploring larger variable and parameter ranges to generalize this approach. This work can be enhanced by readjusting the calibrated parameters and lowering the uncertainty to the extent that measurements of the input variables are available across longer and more spatially dense periods in the basin.

#### 4 Conclusions

This study presented and evaluated a stream temperature modeling approach for the Soil and Water Assessment Tool that integrates an explicit energy balance model to simulate the heat transfer process influenced by riparian shading. The energy balance equation incorporated into the hydrometeorological model included the main sources of energy (shortwave radiation, longwave radiation, evaporation, and conduction). The riparian vegetation was included through the

shade factor in the shortwave radiation equation. An approach for calculating shading factor was proposed and used to evaluate the effects of riparian shading on blocking the solar radiation and reducing the stream temperatures. The capability of the original Ficklin et al. model was improved by enabling mechanisms for capturing the cumulative effects of riparian vegetation shading on the stream temperature within the watershed. Unlike other models, this approach shows the stream temperature simulation at sub-basin scales while considering detailed processes of both heat and mass transfer.

The topographic influence was also assessed, though its influence on the shade factor and the temperature of the streams was found to be very small at the test-bed site. Because of DMW's location in the Northern Hemisphere, solar declination angles during the year were mostly favorable for south-side riparian vegetation to shade E–W- and W–E-oriented streams more than north-side riparian vegetation. Therefore, the contribution of the south-side riparian vegetation to the increase in SF and the reduction in stream temperature was more relevant than the north-side riparian vegetation in E–W- and W–E-oriented streams. Conversely, in S–N- and N–S-oriented streams, shading and contribution of eastern and western banks were similar. Simulations showed that full riparian restoration would reduce the stream temperature on average by 0.91 °C (SD = 0.69 °C) and for efficient restoration by 0.86 °C (SD = 0.67 °C). These reductions were observed mostly in summer than in any other season. In reducing the number of days that exceed 18 °C (biological temperature threshold of aquatic species), full riparian restoration could achieve a reduction in the range of 0 to 58.5 d in the year with an average of 17.1 d. A similar range of reduction could be achieved with the efficient restoration but with a mean of 16.2 d. Lastly, the efficient riparian restoration could be 14.4 % cheaper than the full riparian restoration.

The SWAT model that computes the effects of land management practices on water flow, nutrients, and stream temperature has been successfully applied in several watersheds in the USA and around the world. Similarly, the effectiveness of riparian vegetation in reducing stream temperature was demonstrated in several rivers. Therefore, the application of the improved stream temperature model could be replicated in other regions with characteristics similar to the DMW. However, it is important to note that while the proposed temperature model improves SWAT's ability to simulate riparian buffers as a conservation practice for stream temperature management, this model did not consider the shape of the trees nor the density of the riparian vegetation. Other considerations such as hyporheic exchange processes, frictional heat exchange, and stream geometry that influence stream energy balance were also not incorporated. All of these are recommended directions for future work.

*Data availability.* The data employed in this study are available at <https://doi.org/10.5281/zenodo.6301709> (Noa-Yarasca, 2022).



These data include land cover, soil type, water rights, weather (precipitation, temperature, solar radiation, humidity, and wind speed), flow and stream temperature, modifications to the SWAT rev681 program, and the calibrated DMW SWAT model.

*Supplement.* The supplement related to this article is available online at: <https://doi.org/10.5194/hess-27-739-2023-supplement>.

*Author contributions.* The paper was written by ENY with contributions from all co-authors. ENY collected the data. All authors designed the study. ENY conducted the modeling and analysis. All authors discussed the results and gave critical feedback on the paper.

*Competing interests.* The contact author has declared that none of the authors has any competing interests.

*Disclaimer.* Publisher's note: Copernicus Publications remains neutral with regard to jurisdictional claims in published maps and institutional affiliations.

*Special issue statement.* This article is part of the special issue "Experiments in Hydrology and Hydraulics". It is not associated with a conference.

*Acknowledgements.* This study has been supported by National Oceanic and Atmospheric Administration (Award ID: NA16OAR4320152). We would also like to thank all of our collaborators from the different agencies and institutions: Daniel Sobota at Oregon Department of Environmental Quality, Adriana D. Piemonti, Scott Mansell, and Ting Lu at Clean Water Services, Hillsboro OR, and Sammy Rivera at Oregon State University for the input data and insights provided during this research.

*Financial support.* This research has been supported by the National Oceanic and Atmospheric Administration (grant no. NA16OAR4320152).

*Review statement.* This paper was edited by Carla Ferreira and reviewed by two anonymous referees.

## References

- Abbaspour, K. C., Rouholahnejad, E., Vaghefi, S., Srinivasan, R., Yang, H., and Kløve, B.: A continental-scale hydrology and water quality model for Europe: Calibration and uncertainty of a high-resolution large-scale SWAT model, *J. Hydrol.*, 524, 733–752, <https://doi.org/10.1016/j.jhydrol.2015.03.027>, 2015.
- Abbott, A. G.: The Effect of Riparian Vegetation on Stream Temperature in the Shasta River, University of California, Davis, [http://svrcd.org/wordpress/wp-content/uploads/2012/02/ShastaThesis\\_Final.pdf](http://svrcd.org/wordpress/wp-content/uploads/2012/02/ShastaThesis_Final.pdf) (last access: 20 July 2020, no longer available online), 2002.
- Abdi, R. and Endreny, T.: A river temperature model to assist managers in identifying thermal pollution causes and solutions, *Water (Switzerland)*, 11, 1060, <https://doi.org/10.3390/w11051060>, 2019.
- Abdi, R., Endreny, T., and Nowak, D.: i-Tree cool river: An open source, freeware tool to simulate river water temperature coupled with HEC-RAS, *MethodsX*, 7, 100808, <https://doi.org/10.1016/j.mex.2020.100808>, 2020.
- Albertson, L. K., Ouellet, V., and Daniels, M. D.: Impacts of stream riparian buffer land use on water temperature and food availability for fish, *J. Freshwater Ecol.*, 33, 195–210, <https://doi.org/10.1080/02705060.2017.1422558>, 2018.
- Arnold, J. G., Srinivasan, R., Muttiah, R. S., and Williams, J. R.: Large hydrologic modeling and assessment: Part I. model development, *JAWRA J. Am. Water Resour. As.*, 34, 73–89, 1998.
- Arnold, J. G., Moriasi, D. N., Gassman, P. W., Abbaspour, K. C., White, M. J., Srinivasan, R., Santhi, C., Harmel, R. D., van Griensven, A., van Liew, M. W., Kannan, N., and Jha, M. K.: SWAT: Model use, calibration, and validation, *American Society of Agricultural and Biological Engineers*, 55, 1491–1508, 2012.
- Battin, J., Wiley, M. W., Ruckelshaus, M. H., Palmer, R. N., Korb, E., Bartz, K. K., and Imaki, H.: Projected impacts of climate change on salmon habitat restoration, *P. Natl. Acad. Sci. USA*, 104, 6720–6725, <https://doi.org/10.1073/pnas.0701685104>, 2007.
- Bechtold, W. A.: Crown-Diameter Prediction Models for 87 Species of Stand-Grown Trees in the Eastern United States, *South. J. Appl. For.*, 27, 269–278, <https://doi.org/10.1093/SJAF/27.4.269>, 2003.
- Benyahya, L., Caissie, D., St-Hilaire, A., Ouarda, T. B. M. J., and Bobée, B.: A Review of Statistical Water Temperature Models, *Canadian Water Resour. J.*, 32, 179–192, <https://doi.org/10.4296/cwrj3203179>, 2007.
- Bond, R. M., Stubblefield, A. P., and Van Kirk, R. W.: Sensitivity of summer stream temperatures to climate variability and riparian reforestation strategies, *J. Hydrol.-Reg. Stud.*, 4, 267–279, <https://doi.org/10.1016/j.ejrh.2015.07.002>, 2015.
- Boyd, M.: Heat Source: stream temperature prediction, Oregon State University, Corvallis, OR, [https://ir.library.oregonstate.edu/concern/graduate\\_thesis\\_or\\_dissertations/w95053111](https://ir.library.oregonstate.edu/concern/graduate_thesis_or_dissertations/w95053111) (last access: 10 January 2022), 1996.
- Boyd, M. and Kasper, B.: Analytical Methods for Dynamic Open Channel Heat and Mass Transfer: Methodology for the Heat Source Model Version 7.0, 204 pp., <https://www.oregon.gov/deq/FilterDocs/heatsourcemanual.pdf> (last access: 10 January 2022), 2003.
- Brady, D. K., Graves, W. L., and Geyer, J. C.: Surface heat exchange at power plant cooling lakes, Report No. 5, EEI publication No. 69-901, New York, NY, OSTI: 5095994, 10 pp., 1969.
- Brander, K. M.: Global fish production and climate change, *P. Natl. Acad. Sci. USA*, 104, 19709–19714, <https://doi.org/10.1073/pnas.0702059104>, 2007.
- Brown, G. W.: An improved temperature prediction model for small 15 streams, Oregon State University, Corvallis, OR, <https://ir.library.oregonstate.edu/concern/defaults/6m311t30r?locale=en> (last access: 10 January 2021), 1972.

- Chen, D., Carsel, R., McCutcheon, S., and Nutter, W.: Stream temperature simulation of forested riparian areas: I. watershed-scale model development, *J. Environ. Eng.*, 124, 304–315, [https://doi.org/10.1061/\(ASCE\)0733-9372\(1998\)124:4\(304\)](https://doi.org/10.1061/(ASCE)0733-9372(1998)124:4(304)), 1998a.
- Chen, D., McCutcheon, C., Norton, D. J., and Nutter, W. L.: Stream Temperature Simulation of Forested Riparian Areas: II. Model Application, *J. Environ. Eng.*, 124, 316–328, [https://doi.org/10.1061/\(asce\)0733-9372\(1998\)124:4\(316\)](https://doi.org/10.1061/(asce)0733-9372(1998)124:4(316)), 1998b.
- Curtis, R., Herman, F., and DeMars, D.: Height growth and site index for douglas-fir in high-elevation forests of the Oregon-Washington Cascades, *Forest Sci.*, 20, 307–316, 1974.
- CWL: TMDL Implementation Plan for the City of West Linn, Oregon, City of West Linn, <https://westlinnoregon.gov/publicworks/willamette-tualatin-river-tmdl-plans> (last access: 12 July 2020), 2019.
- Davies-Colley, R. J. and Rutherford, J. C.: Some approaches for measuring and modelling riparian shade, *Ecol. Eng.*, 24, 525–530, <https://doi.org/10.1016/j.ecoleng.2004.01.006>, 2005.
- Davies-Colley, R. J., Meleson, M. A., Hall, R. M. J., and Rutherford, J. C.: Modelling the time course of shade, temperature, and wood recovery in streams with riparian forest restoration, *N. Z. J. Mar. Freshwater Res.*, 43, 673–688, <https://doi.org/10.1080/00288330909510033>, 2009.
- DeWalle, D. R.: Modeling stream shade: Riparian buffer height and density as important as buffer width, *J. Am. Water Resour. Assoc.*, 46, 323–333, <https://doi.org/10.1111/j.1752-1688.2010.00423.x>, 2010.
- Dickey, L. C., McEachran, A. R., Rutherford, C. J., Rehmann, C. R., Perez, M. A., Groh, T. A., and Isenhardt, T. M.: Slope stability of streambanks at saturated riparian buffer sites, *J. Environ. Qual.*, 50, 1430–1439, <https://doi.org/10.1002/jeq2.20281>, 2021.
- Du, X., Shrestha, N. K., Ficklin, D. L., and Wang, J.: Incorporation of the equilibrium temperature approach in a Soil and Water Assessment Tool hydroclimatological stream temperature model, *Hydrol. Earth Syst. Sci.*, 22, 2343–2357, <https://doi.org/10.5194/hess-22-2343-2018>, 2018.
- Dugdale, S. J., Malcolm, I. A., Kantola, K., and Hannah, D. M.: Stream temperature under contrasting riparian forest cover: Understanding thermal dynamics and heat exchange processes, *Sci. Total Environ.*, 610–611, 1375–1389, <https://doi.org/10.1016/j.scitotenv.2017.08.198>, 2018.
- Edinger, J. E., Brady, D. K., and Geyer, J. C.: Heat Exchange and Transport in the Environment, *Electr. Power Res. Inst.*, 14, 125, [https://www.researchgate.net/publication/236539320\\_Heat\\_Exchange\\_and\\_Transport\\_in\\_the\\_Environment](https://www.researchgate.net/publication/236539320_Heat_Exchange_and_Transport_in_the_Environment) (last access: 20 July 2020), 1974.
- Ficklin, D., Luo, Y., Stewart, I. T., and Maurer, E. P.: Development and application of a hydroclimatological stream temperature model within the Soil and Water Assessment Tool, *Water Resour. Res.*, 48, 1511, <https://doi.org/10.1029/2011WR011256>, 2012.
- Ficklin, D. L., Barnhart, B. L., Knouft, J. H., Stewart, I. T., Maurer, E. P., Letsinger, S. L., and Whittaker, G. W.: Climate change and stream temperature projections in the Columbia River basin: habitat implications of spatial variation in hydrologic drivers, *Hydrol. Earth Syst. Sci.*, 18, 4897–4912, <https://doi.org/10.5194/hess-18-4897-2014>, 2014.
- FONDRIEST: Water Temperature, Fundamentals of Environmental Measurements, Fondriest Environmental Learning Center, <https://www.fondriest.com/environmental-measurements/parameters/water-quality/water-temperature/> (last access: 28 October 2021), 2014.
- Fuller, M. R., Leinenbach, P., Detenbeck, N. E., Labiosa, R., and Isaak, D. J.: Riparian vegetation shade restoration and loss effects on recent and future stream temperatures, *Restor. Ecol.*, 30, e13626, <https://doi.org/10.1111/rec.13626>, 2022.
- Garner, G., Malcolm, I. A., Sadler, J. P., and Hannah, D. M.: The role of riparian vegetation density, channel orientation and water velocity in determining river temperature dynamics, *J. Hydrol. (Amst.)*, 553, 471–485, <https://doi.org/10.1016/j.jhydrol.2017.03.024>, 2017.
- Groh, T. A., Isenhardt, T. M., and Schultz, R. C.: Long-term nitrate removal in three riparian buffers: 21 years of data from the Bear Creek watershed in central Iowa, USA, *Sci. Total Environ.*, 740, 140114, <https://doi.org/10.1016/j.scitotenv.2020.140114>, 2020.
- Guenther, S. M., Moore, R. D., and Gomi, T.: Riparian microclimate and evaporation from a coastal headwater stream, and their response to partial-retention forest harvesting, *Agr. Forest Meteorol.*, 164, 1–9, <https://doi.org/10.1016/j.agrformet.2012.05.003>, 2012.
- Hawes, E. and Smith, M.: Riparian Buffer Zones: Functions and Recommended Widths, <https://citeseerx.ist.psu.edu/document?repid=rep1&type=pdf&doi=218d67fc368f96bd7d8a4f92041a3d0aa716a080> (last access: 24 August 2019), 2005.
- Hawksworth, J.: Dairy-McKay Watershed Analysis, Tillamook, <https://www.biodiversitylibrary.org/bibliography/176914> (last access: 22 March 2019), 1999.
- Hebert, C., Caissie, D., Satish, M. G., and El-Jabi, N.: Study of stream temperature dynamics and corresponding heat fluxes within Miramichi River catchments (New Brunswick, Canada), *Hydrol. Process.*, 25, 2439–2455, <https://doi.org/10.1002/hyp.8021>, 2011.
- Hennings, R. B.: Stream Temperature Management in the Tualatin Watershed: Is it Improving Salmonid Habitat?, Portland State University, Geography Masters Research Papers, 8, [https://pdxscholar.library.pdx.edu/geog\\_masterpapers/8/](https://pdxscholar.library.pdx.edu/geog_masterpapers/8/) (last access: 12 May 2019), 2014.
- Hernandez-Santana, V., Asbjornsen, H., Sauer, T., Isenhardt, T., Schilling, K., and Schultz, R.: Enhanced transpiration by riparian buffer trees in response to advection in a humid temperate agricultural landscape, *Forest Ecol. Manag.*, 261, 1415–1427, <https://doi.org/10.1016/j.foreco.2011.01.027>, 2011.
- Hester, E. T. and Doyle, M. W.: Human Impacts to River Temperature and Their Effects on Biological Processes: A Quantitative Synthesis, *JAWRA J. Am. Water Resour. As.*, 47, 571–587, <https://doi.org/10.1111/j.1752-1688.2011.00525.x>, 2011.
- Hill, W. R., Ryon, M. G., and Schilling, E. M.: Light Limitation in a Stream Ecosystem: Responses by Primary Producers and Consumers, *Ecology*, 76, 1297–1309, <https://doi.org/10.2307/1940936>, 1995.
- Iman, R. L.: Latin Hypercube Sampling, in: Wiley Stats. Ref: Statistics Reference Online, edited by: Balakrishnan, N., Colton, T., Everitt, B., Piegorisch, W., Ruggeri, F., and Teugels, J. L., <https://doi.org/10.1002/9781118445112.stat03803>, 2014.

- Isaak, D. J., Wollrab, S., Horan, D., and Chandler, G.: Climate change effects on stream and river temperatures across the north-west U.S. from 1980–2009 and implications for salmonid fishes, *Clim. Change*, 113, 499–524, <https://doi.org/10.1007/s10584-011-0326-z>, 2012.
- Ishikawa, M., Haag, I., Krumm, J., Teltscher, K., and Lorke, A.: The effect of stream shading on the inflow characteristics in a downstream reservoir, *River Res. Appl.*, 37, 943–954, <https://doi.org/10.1002/rra.3821>, 2021.
- Jackson, F. L., Hannah, D. M., Ouellet, V., and Malcolm, I. A.: A deterministic river temperature model to prioritize management of riparian woodlands to reduce summer maximum river temperatures, *Hydrol. Process.*, 35, 1–19, <https://doi.org/10.1002/hyp.14314>, 2021.
- Johnson, M. and Wilby, R.: Seeing the landscape for the trees: Metrics to guide riparian shade management in river catchments, *Water Resour. Res.*, 51, 3754–3769, <https://doi.org/10.1002/2014WR016802>, 2015.
- Kalny, G., Laaha, G., Melcher, A., Trimmel, H., Weihs, P., and Rauch, H. P.: The influence of riparian vegetation shading on water temperature during low flow conditions in a medium sized river, *Knowl. Manag. Aquat. Ecosyst.*, 418, 5, <https://doi.org/10.1051/kmae/2016037>, 2017.
- Kałuża, T., Sojka, M., Wróżyński, R., Jaskuła, J., Zaborowski, S., and Hämmerling, M.: Modeling of river channel shading as a factor for changes in hydromorphological conditions of small lowland rivers, *Water*, 12, 527, <https://doi.org/10.3390/w12020527>, 2020.
- Kaushal, S. S., Likens, G. E., Jaworski, N. A., Pace, M. L., Sides, A. M., Seekell, D., Belt, K. T., Secor, D. H., and Wingate, R. L.: Rising stream and river temperatures in the United States, *Front. Ecol. Environ.*, 8, 461–466, <https://doi.org/10.1890/090037>, 2010.
- Kim, K. and Chapra, S.: Temperature model for highly transient shallow streams, *J. Hydraul. Eng.*, 123, 30–40, 1997.
- Koh, I., Kim, S., and Lee, D.: Effects of bibosooop plantation on wind speed, humidity, and evaporation in a traditional agricultural landscape of Korea: Field measurements and modeling, *Agr. Ecosyst. Environ.*, 135, 294–303, <https://doi.org/10.1016/j.agee.2009.10.008>, 2010.
- Krause, P., Boyle, D. P., and Båse, F.: Comparison of different efficiency criteria for hydrological model assessment, *Adv. Geosci.*, 5, 89–97, <https://doi.org/10.5194/adgeo-5-89-2005>, 2005.
- LANDFIRE: Existing Vegetation Type Layer, LANDFIRE 2.0.0, U.S. Department of the Interior, Geological Survey, and U.S. Department of Agriculture, <https://www.landfire.gov/viewer/> (last access: 28 October 2021), 2019.
- Lawrence, M. G.: The relationship between relative humidity and the dewpoint temperature in moist air: A simple conversion and applications, *B. Am. Meteorol. Soc.*, 86, 225–233, <https://doi.org/10.1175/BAMS-86-2-225>, 2005.
- LeBlanc, R. T. and Brown, R. D.: The Use of Riparian Vegetation in Stream-Temperature Modification, *Water Environ. J.*, 14, 297–303, <https://doi.org/10.1111/j.1747-6593.2000.tb00264.x>, 2000.
- Li, G., Jackson, C. R., and Kraseski, K. A.: Modeled riparian stream shading: Agreement with field measurements and sensitivity to riparian conditions, *J. Hydrol. (Amst.)*, 428–429, 142–151, <https://doi.org/10.1016/j.jhydrol.2012.01.032>, 2012.
- Liao, J., Wang, T., Wang, X., Xie, M., Jiang, Z., Huang, X., and Zhu, J.: Impacts of different urban canopy schemes in WRF/Chem on regional climate and air quality in Yangtze River Delta, China, *Atmos. Res.*, 145–146, 226–243, <https://doi.org/10.1016/j.atmosres.2014.04.005>, 2014.
- Liu, K., Yang, R., Lu, J., Wang, X., Lu, B., Tian, X., and Zhang, Y.: Radiation use efficiency and source-sink changes of super hybrid rice under shade stress during grain-filling stage, *Agron. J.*, 111, 1788–1798, <https://doi.org/10.2134/agronj2018.10.0662>, 2019.
- Lutz, S. R., Trauth, N., Musolff, A., van Breukelen, B. M., Knöller, K., and Fleckenstein, J. H.: How Important is Denitrification in Riparian Zones? Combining End-Member Mixing and Isotope Modeling to Quantify Nitrate Removal from Riparian Groundwater, *Water Resour. Res.*, 56, e2019WR025528, <https://doi.org/10.1029/2019WR025528>, 2020.
- Malkinson, D. and Wittenberg, L.: Scaling the effects of riparian vegetation on cross-sectional characteristics of ephemeral mountain streams—a case study of Nahal Oren, Mt. Carmel, Israel, *Catena (Amst.)*, 69, 103–110, <https://doi.org/10.1016/j.catena.2006.04.026>, 2007.
- Marteau, B., Piégay, H., Chandesris, A., Michel, K., and Vaudor, L.: Riparian shading mitigates warming but cannot revert thermal alteration by impoundments in lowland rivers, *Earth Surf. Proc. Land.*, 47, 2209–2229, <https://doi.org/10.1002/esp.5372>, 2022.
- Minnesota Board of Water and Soil Resources: Wetlands Restoration Strategy, <https://bwsr.state.mn.us/wetland-restoration-0> (last access: 23 June 2019), 2009.
- Mohseni, O. and Stefan, H. G.: Stream temperature/air temperature relationship: A physical interpretation, *J. Hydrol. (Amst.)*, 218, 128–141, [https://doi.org/10.1016/S0022-1694\(99\)00034-7](https://doi.org/10.1016/S0022-1694(99)00034-7), 1999.
- Moriassi, D. N., Arnold, J. G., van Liew, M. W., Binger, R. L., Harmel, R. D., and Veith, T. L.: Model evaluation guidelines for systematic quantification of accuracy in watershed simulations, *American Society of Agricultural and Biological Engineers*, 50, 885–900, <https://doi.org/10.13031/2013.23153>, 2007.
- Morin, G. and Couillard, D.: Predicting river temperatures with a hydrological model, in: *Encyclopedia of Fluid Mechanics, Surface and Groundwater Flow Phenomena*, in: *Encyclopedia of Fluid Mechanics: Surface and Groundwater Flow Phenomena*, Texas, 171–209, ISBN 13 978-0872015449, 1990.
- Mustafa, M., Barnhart, B., Babbar-Sebens, M., and Ficklin, D.: Modeling landscape change effects on stream temperature using the Soil and Water Assessment Tool, *Water (Switzerland)*, 10, 1–17, <https://doi.org/10.3390/w10091143>, 2018.
- National Park Services: Periphyton. Big Cypress, National Preserve Florida, <https://www.nps.gov/bicy/learn/nature/periphyton.htm> (last access: 20 July 2022), 2020.
- Neitsch, S. L., Arnolds, J. G., Kiniry, J. R., and Williams, J. R.: Soil and water assessment tool, theoretical documentation (Version 2009), <https://swat.tamu.edu/media/99192/swat2009-theory.pdf> (last access: 22 September 2018), 2009.
- Nelitz, M. A., MacIsaac, E. A., and Peterman, R. M.: A Science-Based Approach for Identifying Temperature-Sensitive Streams for Rainbow Trout, *N. Am. J. Fish Manage.*, 27, 405–424, <https://doi.org/10.1577/M05-146.1>, 2007.
- NMFS: Recovery plan for the evolutionarily significant unit of Central California Coast Coho salmon, United States, National Marine Fisheries Service; United States, National Marine Fisheries

- Service, Southwest Region, Volume 1, <https://repository.library.noaa.gov/view/noaa/15987> (last access: 24 October 2019), 2012.
- NMFS: Final recovery plan for the Southern Oregon/Northern California Coast evolutionarily significant unit of Coho salmon (*Oncorhynchus kisutch*). United States, National Marine Fisheries Service; United States, National Marine Fisheries Service, West Coast Region, <https://repository.library.noaa.gov/view/noaa/15985> (last access: 24 October 2019), 2014.
- Noa-Yarasca, E.: SF\_model/Shade Factor for the modified Ficklin stream temperature model, GitHub [code], [https://github.com/noayarae/SF\\_model.git](https://github.com/noayarae/SF_model.git) (last access: 10 November 2021), 2021.
- Noa-Yarasca, E.: Data on An Improved Model of Shade-affected Stream Temperature in Soil & Water Assessment Tool, Zenodo [data set], <https://doi.org/10.5281/zenodo.6301709>, 2022.
- Nguyen, D.: Warming rivers in US West killing fish, imperiling industry, AP NEWS, <https://apnews.com/article/business-environment-and-nature-fish-climate-change-5c85e86a2ba18171ca55d5de8f89dea3> (last access: 28 October 2021), 2021.
- ODA: Tualatin River Watershed Agricultural Water Quality Management Area Plan, Tualatin River Watershed Local Advisory Committee Oregon Department of Agriculture, Portland, Oregon, <https://www.oregon.gov/oda/shared/Documents/Publications/NaturalResources/TualatinAWQMAreaPlan.pdf> (last access: 12 November 2020), 2018.
- ODEQ: Tualatin subbasin Total Maximum Daily Load (TMDL). Oregon Department of Environmental Quality, <https://www.oregon.gov/deq/FilterDocs/tmdlwqmp.pdf> (last access: 20 July 2019), 2001.
- ODEQ: Temperature Water Quality Standard Implementation. A DEQ Internal Management Directive. Oregon Department of Environmental Quality, State of Oregon, <https://www.oregon.gov/deq/FilteredLibrary/IMDTemperature.pdf> (last access: 20 July 2019), 2008.
- ODEQ: Cost Estimate to Restore Riparian Forest Buffers and Improve Stream Habitat in the Willamette Basin, Oregon, Department of Environmental Quality, State of Oregon, Portland, 52 pp., <https://www.oregon.gov/deq/wq/Documents/willRipCostRev2.pdf> (last access: 20 July 2019), 2010.
- PRISM Climate Group: PRISM Climate Data, PRISM Climate Group, Oregon State University, <https://prism.oregonstate.edu> (last access: 23 May 2019), 2014.
- USBR: Columbia-Pacific Northwest Region, <https://www.usbr.gov/pn/agrimet/wxdata.html>, last access: 10 December 2020.
- OWRD: Water Rights Oregon Water Resources Department, <https://www.oregon.gov/owrd/programs/WaterRights/Pages/default.aspx>, last access: 7 January 2021.
- Parish, O. O. and Putnam, T. W.: Equations for the Determination of Humidity from Dewpoint and Psychrometric data, Washington, D.C., [https://www.nasa.gov/centers/dryden/pdf/87878main\\_H-937.pdf](https://www.nasa.gov/centers/dryden/pdf/87878main_H-937.pdf) (last access: 12 May 2020), 1977.
- Parkyn, S.: Review of Riparian Buffer Zone Effectiveness, New Zealand, ISBN 0-478-07823-4, 2004.
- Poole, G. C. and Berman, C. H.: An Ecological Perspective on In-Stream Temperature: Natural Heat Dynamics and Mechanisms of Human-Caused Thermal Degradation, *Environ. Manage.*, 27, 787–802, <https://doi.org/10.1007/s002670010188>, 2001.
- Risley, J. C., Roehl, E. A., and Conrads, P. A.: Estimating Water Temperatures in Small Streams in Western Oregon Using Neural Network Models, Portland, Oregon, <https://pubs.usgs.gov/wri/wri024218/> (last access: 22 January 2021), 2003.
- Rodrigues, I. S., Costa, C. A. G., Raabe, A., Medeiros, P. H. A., and de Araújo, J. C.: Evaporation in Brazilian dryland reservoirs: Spatial variability and impact of riparian vegetation, *Sci. Total Environ.*, 797, 149059, <https://doi.org/10.1016/j.scitotenv.2021.149059>, 2021.
- Roth, T. R., Westhoff, M. C., Huwald, H., Huff, J. A., Rubin, J. F., Barrenetxea, G., Vetterli, M., Parriaux, A., Selker, J. S., and Parlange, M. B.: Stream temperature response to three riparian vegetation scenarios by use of a distributed temperature validated model, *Environ. Sci. Technol.*, 44, 2072–2078, <https://doi.org/10.1021/es902654f>, 2010.
- Rothwell, E. L.: the Influence of Hyporheic Flow on Stream Temperature, Boise State University, <https://scholarworks.boisestate.edu/td/402/> (last access: 22 January 2021), 2005.
- Rutherford, J. C., Blackett, S., Blackett, C., Saito, L., and Davies-Colley, R. J.: Predicting the effects of shade on water temperature in small streams, *N. Z. J. Mar. Freshwater Res.*, 31, 707–721, <https://doi.org/10.1080/00288330.1997.9516801>, 1997.
- Sahatjian, B.: Modeling Effective Shade to Prioritize Riparian Restoration Efforts in the Johnson Creek Watershed, Portland State University, [https://pdxscholar.library.pdx.edu/mem\\_gradprojects/42/](https://pdxscholar.library.pdx.edu/mem_gradprojects/42/) (last access: 28 May 2021), 2013.
- Schiller, D. von, Marti, E., Riera, J. L., and Sabater, F.: Effects of nutrients and light on periphyton biomass and nitrogen uptake in Mediterranean streams with contrasting land uses, *Freshwater Biol.*, 52, 891–906, <https://doi.org/10.1111/j.1365-2427.2007.01742.x>, 2007.
- Seyedhashemi, H., Vidal, J.-P., Diamond, J. S., Thiéry, D., Monteil, C., Hendrickx, F., Maire, A., and Moatar, F.: Regional, multi-decadal analysis on the Loire River basin reveals that stream temperature increases faster than air temperature, *Hydrol. Earth Syst. Sci.*, 26, 2583–2603, <https://doi.org/10.5194/hess-26-2583-2022>, 2022.
- Sherwood, C.: Thousands of salmon die in hotter-than-usual Northwest rivers; Reuters, <https://www.reuters.com/article/us-oregon-salmon/thousands-of-salmon-die-in-hotter-than-usual-northwest-rivers-idUSKCN0Q203P20150728> (last access: 20 July 2021), 2015.
- Sohrabi, M. M., Benjankar, R., Tonina, D., Wenger, S. J., and Isaak, D. J.: Estimation of daily stream water temperatures with a Bayesian regression approach, *Hydrol. Process.*, 31, 1719–1733, <https://doi.org/10.1002/hyp.11139>, 2017.
- Spanjer, A. R., Gendaszek, A. S., Wulfkuhle, E. J., Black, R. W., and Jaeger, K. L.: Assessing climate change impacts on Pacific salmon and trout using bioenergetics and spatiotemporal explicit river temperature predictions under varying riparian conditions, *PLoS One*, 17, e0266871, <https://doi.org/10.1371/journal.pone.0266871>, 2022.
- Stefan, H. G. and Preud'homme, E. B.: Stream Temperature Estimation From Air Temperature, *JAWRA J. Am. Water Resour. As.*, 29, 27–45, <https://doi.org/10.1111/j.1752-1688.1993.tb01502.x>, 1993.
- Temesgen, H., Hann, D. W., and Monleon, V. J.: Regional height-diameter equations for major tree species of southwest Oregon, 22, 213–219, *West. J. Appl. For.*, 22, 213–219, <https://doi.org/10.1093/WJAF/22.3.213>, 2007.

- Thomas, S. C. and Winner, W. E.: Leaf area index of an old-growth Douglas-fir forest estimated from direct structural measurements in the canopy, *Can. J. Forest Res.*, 30, 1922–1930, <https://doi.org/10.1139/x00-121>, 2000.
- USDA: Geospatial Data Gateway, <https://datagateway.nrcs.usda.gov/>, last access: 20 July 2019.
- USGS: National Water Information System Web Interface, <https://waterdata.usgs.gov/nwis>, last access: 28 October 2019b.
- White, S. M., Justice, C., Kelsey, D. A., McCullough, D. A., and Smith, T.: Legacies of stream channel modification revealed using General Land Office surveys, with implications for water temperature and aquatic life, *Elementa*, 5, 3, <https://doi.org/10.1525/elementa.192>, 2017.
- Wigmosta, M. S., Vail, L. W., and Lettenmaier, D. P.: A distributed hydrology-vegetation model for complex terrain, *Water Resour. Res.*, 30, 1665–1679, <https://doi.org/10.1029/94WR00436>, 1994.
- Winfrey, M. M., Hood, E., Stuefer, S. L., Schindler, D. E., Cline, T. J., Arp, C. D., and Pyare, S.: Landcover and geomorphology influence streamwater temperature sensitivity in salmon bearing watersheds in Southeast Alaska, *Environ. Res. Lett.*, 13, 064034, <https://doi.org/10.1088/1748-9326/aac4c0>, 2018.
- Wondzell, S. M., Diabat, M., and Haggerty, R.: What Matters Most: Are Future Stream Temperatures More Sensitive to Changing Air Temperatures, Discharge, or Riparian Vegetation?, *JAWRA J. Am. Water Resour. As.*, 55, 116–132, <https://doi.org/10.1111/1752-1688.12707>, 2019.
- Yearsley, J. R.: A semi-Lagrangian water temperature model for advection-dominated river systems, *Water Resour. Res.*, 45, 1–19, <https://doi.org/10.1029/2008WR007629>, 2009.
- Zhu, S., Du, X., and Luo, W.: Incorporation of the simplified equilibrium temperature approach in a hydrodynamic and water quality model – CE-QUAL-W2, *Water Sci. Technol. Water Supply*, 19, 156–164, <https://doi.org/10.2166/ws.2018.063>, 2019.